frontiers | Frontiers in Sustainability

TYPE Original Research
PUBLISHED 08 November 2022
DOI 10.3389/frsus.2022.941131

OPEN ACCESS

EDITED BY
Krzysztof Urbaniec,
Warsaw University of Technology, Poland

REVIEWED BY
Karna Wijaya,
Gadjah Mada University, Indonesia
Jaroslaw Serafin,
Universitat Politecnica de Catalunya, Spain

*CORRESPONDENCE
Juan Carlos Moreno-Piraján
jumoreno@uniandes.edu.co

SPECIALTY SECTION
This article was submitted to Sustainable Chemical Process Design, a section of the journal Frontiers in Sustainability

RECEIVED 11 May 2022
ACCEPTED 30 August 2022
PUBLISHED 08 November 2022

CITATION
Martínez Gil JM, Vivas-Reyes R, Bastidas-Barranco MJ, Giraldo L and Moreno-Piraján JC (2022) Evaluation of biocatalysts synthesized with lipase from *Pseudomonas cepacia* supported on glycol-modified MOF-199 in the synthesis of green biodiesel. *Front. Sustain.* 3:941131. doi: 10.3389/frsus.2022.941131

Evaluation of biocatalysts synthesized with lipase from *Pseudomonas cepacia* supported on glycol-modified MOF-199 in the synthesis of green biodiesel

José Manuel Martínez Gil[1,2,3,4], Ricardo Vivas-Reyes[2], Marlón José Bastidas-Barranco[3], Liliana Giraldo[5] and Juan Carlos Moreno-Piraján[4]*

[1]Grupo de Investigación Catálisis y Materiales, Facultad de Ciencias Básicas y Aplicadas, Universidad de La Guajira, Riohacha, Colombia, [2]Grupo de Investigación Química Cuántica y Teórica, Facultad de Ciencias Exactas y Naturales, Universidad de Cartagena, Cartagena, Colombia, [3]Grupo de Investigación Desarrollo de Estudios y Tecnologías Ambientales del Carbono (DESTACAR), Facultad de Ingenierías, Universidad de La Guajira, Riohacha, Colombia, [4]Grupo de Investigación en Sólidos Porosos y Calorimetría, Facultad de Ciencias, Departamento de Química, Universidad de los Andes, Bogotá, Colombia, [5]Grupo de Calorimetría, Facultad de Ciencias, Departamento de Química, Universidad Nacional de Colombia, Bogotá, Colombia

In this work, we report the synthesis and characterization of biocatalysts prepared using MOF-199 and lipase from *Pseudomonas cepacia* as a support, an agent for the breakdown of saturated, monounsaturated, and polyunsaturated fatty acids, the main components of palm oil (*Elaeis guineensis*), used to produce green biodiesel. Lipase from *Pseudomonas cepacia* (PCL) is used as an enzyme, which is supported by adsorption on MOF-199 (MOF-199-PCL) and another part of MOF-199 is modified with glycol as a carbon source to which PCL is supported to obtain the modified MOF (Gly@MOF-199-PCL). MOF-199 was modified by calcining a sample at 900°C for 2 h at a heating rate of 7°C/min, in an inert atmosphere and then stored in a desiccator to protect it from moisture before proceeding to adsorb PCL. Both the biocatalysts (MOF-199-PCL and Gly@MOF-199-PCL) and the supernatant liquid were characterized using Fourier transform infrared spectroscopy (FTIR), Raman spectroscopy, energy dispersive X-ray spectroscopy (EDS or EDX), gas chromatography coupled with mass (GC-MS), and nuclear magnetic resonance (NMR). The results of the instrumental part show that both biocatalysts produce green biodiesel, which is a novel contribution to these systems.

KEYWORDS

metal-organic framework, adsorption, green biodiesel, lipases, biocatalysts

Introduction

In the context of the elaboration of catalytic materials for transesterification reactions for biodiesel, the synthesis of catalysts that satisfy the problems generated by the homogeneous and heterogeneous catalysts used for both acid and base catalysis becomes pertinent. Metal-organic structures (MOFs) appear in this scenario, a class of porous ordered materials discovered by Prof. Omar Yaghi (Al Obeidli et al., 2021) that combine some of the best characteristics of both homogeneous catalysts and can provide structures with varying amounts of basic and acidic active sites. Among these compounds is MOF-199, which is characterized by the presence of Cu^{2+} ion nuclei in its structure surrounded by benzene-1,3,5-tricarboxylic acid ligands. This MOF has been used in biodiesel synthesis due to its ability to act in esterification and/or transesterification reactions with or without modifications. However, compared to basic catalysts, MOF-199 does not exhibit high performance as a heterogeneous catalyst in transesterification reactions of oils and/or fats in biodiesel production processes. In this scenario, enzymes emerge as promising materials for the development of new technologies leading to the production of biodiesel. Enzymes consume less activation energy than mass catalysts because the reactions mediated by these biocatalysts occur under low conditions and can be applied to a wide range of substrates (Kumar et al., 2020). Additionally, enzymatic catalysis does not require high-quality raw materials, since enzymes do not react with impurities (Angulo et al., 2020). In this context, there are enzymes with a high affinity for lipid substrates, these enzymes are called lipolytic, among which lipases stand out (Kovacic et al., 2019), because they can hydrolyze long-chain fatty acid acylglycerols into glycerol and fatty acids step by step and in turn can transform fatty acids into esters. Additionally, lipases are soluble in water, and therefore, at the oil–water interface, they present better catalytic activity (Shomal et al., 2022). Among the liquid lipases, those produced by the species *Pseudomonas cepacia* have drawn attention because in comparison to the other enzymes, they are low in cost, tolerate methanol, esterify free fatty acids, and have a high biodiesel conversion (Chang et al., 2021; Shomal et al., 2022). Despite the benefits presented by the *Pseudomonas cepacia* lipase, drawbacks such as its high resistance to mass transfer, the tendency to adsorb glycerol in the reaction medium, and the low operational stability still remain to be overcome (Shomal et al., 2021). These drawbacks can be overcome with the immobilization of lipases on MOF-type support. The anchoring of the lipase ensures its reuse and it also improves: activity, selectivity or specificity, stability to drastic conditions, and the purity of the lipase (Monteiro et al., 2021). For its part, MOF-199 is an excellent candidate as a support for *Pseudomonas cepacia* lipase, because compared to other MOFs, it produces a greater amount of biodiesel without affecting catalytic activity (Shomal et al., 2021, 2022). Despite these characteristics, MOFs as catalytic support for lipase anchoring have the drawback that coordination interactions are weak (Wang et al., 2019); for this reason, their modification is necessary before using them as an immobilizer for *Pseudomonas cepacia* enzymes. In addition to the previously mentioned catalysts, the synthesis of catalysts that allow the incorporation of glycerin as a component of biodiesel in the form of monoglycerides aids in the reduction of impurities (Heiden et al., 2021), thus improving the biofuel's quality (Krishnasamy and Bukkarapu, 2021). The addition of glycerol to the mixture of fatty acid methyl esters (FAMEs) in biodiesel is formulated as Ecodiesel and has the advantage of increasing the lubricity (Milano et al., 2022) of the energy solution. In addition to the above, catalysts that incorporate residual products or by-products such as paraffins into the green diesel mixture are required. The incorporation of high molecular weight aliphatic hydrocarbons into the renewable mixture increases the number of rye and thus the efficiency of combustion (Zhen et al., 2020). If a material overcomes the above drawbacks, it would still not be classified as an excellent catalyst, since it must be capable of carrying out transesterification reactions and esterification reactions simultaneously. In order to contribute to the solution of the problems associated with the production of biodiesel, in this study biocatalysts were synthesized and characterized from the immobilization of *Pseudomonas cepacia* lipases on MOF-199 modified with ethylene glycol, as an alternative that seeks to overcome the limitations presented by acid and basic catalysts used in the process of obtaining biodiesel.

Experimental methodology

Reagents used

MOF-199 (Sigma-Aldrich), lipase from *Pseudomonas cepacia* [Sigma-Aldrich (62309)], methyl alcohol (R.A. Carlo Erba^{TM}), ethylene glycol (R.A. Carlo Erba^{TM}), KOH (R.A., Carlo Erba^{TM} brand), 0.1 M solution of CH_3COOH, buffer at pH 7, commercial biodiesel (BIOC), African Palm Oil (PO) (certified by the National Federation of Oil Growers, FedePalma), commercial Glycerin (GC), and glycerin obtained from palm oil by basic catalysis (BC-OP-BIO).

Modification of MOF-199 with ethylene glycol

In order to allow the anchoring of the *Pseudomonas cepacia* lipase in the MOF structure. MOF-199 was modified by the impregnation method using ethylene glycol as a carbon source (Zhao et al., 2022): 0.9944 g of MOF-199 was taken and 12.5 ml of ethylene glycol was added. The mixture obtained

TABLE 1 Quantities of starting materials to obtain biocatalysts.

Support	Active site		
Initials	Mass (g)	Name	Mass (g)
*MOF-199	0.1114	*Pseudomonas cepacia*	0.0306
**Gly@MOF-199	0.0372	*Pseudomonas cepacia*	0.0376

The new catalytic materials were labeled * MOF-199-PCL and ** Gly@MOF-199-PCL.

was left in contact for 13 days (Wang et al., 2019). After this interaction time, the MOF-199 impregnated with ethylene glycol was calcined in order to modify it. The new material was named Gly@MOF-199. The calcination conditions to obtain the Gly@MOF-199 were the following; ramp I: initial temperature 40°C, final temperature 200°C for 1 h, with heating rate 3°C/min; ramp II: initial temperature 200°C, and final temperature 900°C for three and a half hours (3.30 h), with a heating rate of 7°C/min.

Impregnation of MOF-199 and Gly@MOF-199 with *Pseudomonas cepacia* lipase

Two (2) solutions were prepared using the following materials as solute: MOF-199, Gly@MOF-199, and *Pseudomonas cepacia* samples using a buffer at pH 7. The lipase support ratio for the case of MOF-199 was 1:4 and for the case of Gly@MOF-99, it was 1:1, because the MOF-199 support has a greater surface area than its derivative, Gly@MOF-199. The amounts of preparation of the solutions are shown in Table 1. The solutions were left to cool for 24 h at a temperature of −80°C, and then they were lyophilized.

Derivatization of palm oil for mass analysis

The derivatization method with BF_3:MeOH (∼10%) and sodium methoxide was performed with 300 μl of a methanolic solution of the sample at 500 ppm concentration, containing methyl nonanoate at 300 ppm as internal standard (IS). About 100 μl of sodium methoxide were added to the above solution and heated at 50°C in an oil bath for 10 min. Subsequently, 180 μl of BF_3:MeOH solution (10% approx.) is added and it is heated again in an oil bath at 50°C for an additional 16 mins. For the extraction, they were added in the following order: 200 μl of water and 200 μl of GC-grade hexane. It was vortexed for 30 s and centrifuged at 5,000 rpm for 5 mins, collecting the upper organic phase, transferring to a 2 ml vial with a 300 μl insert, and injecting it into the gas chromatograph coupled with a mass analyzer (GC-MS) for the analysis of fatty acid methyl esters (FAMEs).

TABLE 2 Mass of supports used to immobilize lipase from *Pseudomonas cepacia*.

Catalyst	Mass (g)
MOF-199-PCL	0.1287
Gly@MOF-199	0.0758

Preparation of sodium methoxide:

$$CH_3OH + Na \rightarrow CH_3ONa$$

About 574.8 mg of Na were taken and reacted with 50 ml of methanol. Then, the method described above was applied, leaving the derivatizations ready for analysis.

Transesterification reaction: Supported *Pseudomonas cepacia* lipase + methanol

Samples of MOF-199-PCL and Gly@MOF-199-PCL were stored in a moisture-free environment until they were used and then introduced as biocatalysts in transesterification reactions. Methanol was used as solvent and African palm oil (OP) as raw material. The specifications for the process were the following:

Quantities of MOF-199-PCL and Gly@MOF-199-PCL were taken separately, as indicated in Table 2, 1 ml of palm oil and 4 ml of methanol were added to each reactor and left to react for 24 h. After this time, 1 ml of methanol was added to each reactor and it was left to react for 24 h. After this time, the biodiesel was separated from the other phases.

To compare the biodiesel synthesized with the biocatalysts (MOF-199-PCL and Gly@MOF-199-PCC) and that obtained by the transesterification of palm oil using potassium methoxide in a 1:20 ratio and allowed to react in a reactor with constant stirring at 250 rpm for a week at room temperature. Once the biodiesel is obtained, the phases are separated, and then it is neutralized with 0.1 molar acetic acid. Once the biodiesel was neutralized, the excess water was separated by heating to 5°C every 20 mins.

Biodiesel-based products were labeled as:

a. Commercial biodiesel obtained from palm oil (OP-BIOC);
b. Biodiesel obtained by basic catalysis (BC-OP-BIO);
c. Biodiesel obtained by MOF-199-PCL (BIO-MOF-199-PCL);
d. Biodiesel obtained by Gly@MOF-199-PCL (BIO-Gly@MOF-199-PCL).

Fourier transform infrared spectrophotometry

The Fourier transform infrared spectrophotometry (FTIR) absorbance spectra of Gly@MOF-199 and Gly@MOF-199-PCL were obtained using the diffuse reflectance technique (Fuller and Griffiths, 1978), with analysis performed on an IRTracer-100 Shimadzu spectrometer in the range of wavenumbers of 4,000–400 cm^{-1}. The solid samples were mixed with KBr in a ratio of ∼1/300, and then the mixture was ground in an agate mortar to a very fine powder. The FTIR absorbance spectrum of Gly@MOF-199 was obtained using the KBr technique. After drying at 100°C for 12 h in a vacuum oven, about 300 mg of the fine powder was used to make a pellet. After preparation, the pellet was immediately analyzed and the spectra were recorded by a series of scans with a resolution of 4 cm^{-1}. A pellet prepared with an equivalent amount of pure KBr powder was used as background. FTIR absorbance spectra for MOF-199, palm oil, OP-BIOC, BC-OP-BIO, BIO-MOF-199-PCL, BIO-Gly@MOF-199-PCL, glycerin GC, and glycerin GOP-CB were obtained using the attenuated total reflectance (ATR) technique.

TABLE 3 Biodiesel solutions at 5,000 ppm, for GC-MS.

	Biodiesel		Metanol
No.	Nomenclature	Mass (g)	
1	OP. BIOC	0.0521	1 ml
2	BC-OP-*BIO*	0.0547	
3	BIOMOF-199-PCL	0.055	
4	BIOGly@MOF-199-PCL	0.0500	

Gas chromatography coupled to masses

In order to separate, analyze and quantify the acylglycerol present in palm oil and the fatty acid methyl ester components in the biodiesel obtained, a GC System gas chromatograph was used. Solutions were prepared at 5,000 ppm of each biodiesel in methanol using a Hewlett Packard coupled with a Mass Selective Detector Agilent Technologies 5973 Network mass spectrometer, then each solution was brought to 1,000 ppm by taking 0.020 µl of the mother solutions and adding 980 µl of chloroform, as shown in Table 3.

Separation was performed on a DB-5MS capillary column (30 m × 0.32 mm, 0.25 µm thick). The carrier gas was helium with a flow rate of 1.5 ml/min. The column temperature was programmed from 120 to 300°C at a rate of 10°C/min. The temperature of both the injector and the detector was set at 250°C. A sample volume of 1 µl of dichloromethane as blank was injected, using a split mode, with a split ratio of 1:10. The mass spectrometer was configured to scan in the range of m/z 40.00–300.00 with electron impact ionization (El) mode.

Raman microscopy

The determination of the chemical structure of the materials MOF-199, Gly@MOF-199, MOF-199-PCL, and Gly@MOF-199-PCL by Raman spectroscopy was carried out using a Raman Spectrometer-Confocal Raman XploRA^{TM}PLUS microscope. A laser line with 532 nm as excitation source, grating of 1,200 lines per mm, and slit openings of 11 and 65 µm was applied to operate in the confocal mode. The nominal spectral resolution was 2 $cm^{-1.}$ Finely divided solid samples were manually placed at the focal point within the glass slide to minimize

TABLE 4 Nomenclature of the substances used and products obtained in the production of biodiesel from the immobilization of *Pseudomonas cepacia* in MOF-199.

Process	Type of substance	Synthesized samples	
		Nomenclature	Study analysis technique
Synthesis of catalytic materials	Starting material	MOF-199	FTIR
		Gly@MOF-199	RAMAN
	Biocatalysts	MOF-199-PCL	SEM-EDS
		Gly@MOF-199-PCL	
Biofuel synthesis	Starting material	OP	FTIR
		OP-BIOC	CG-MS
	Comparative materials	BC-OP-*BIO*	RMN
		Glycerine GC	
		Glycerine GOP-CB	
	Biodiesel	BIO-MOF-199-PCL	
		BIO-Gly@MOF-199-PCL	

contributions from the glass walls and maximize signal from the reaction medium.

Morphological analysis semi-quantitative chemical composition (SEM-EDS)

The morphological characterization of MOF-199, Gly@MOF199, MOF-199-PCL, and Gly@MOF-199-PCL was evaluated with the help of a scanning electron microscope. JEOL scanning electron microscope, model JSM 6490-LV connected to the microprobe technique (EDS) in EDX mode; for this purpose, the finely divided solids were homogenized in relation to particle size and covered with a thin film of gold /deposited by chemical vapor deposition (CVD). Images were obtained at magnifications between 2,500 and 20,000×.

Nuclear magnetic resonance

The NMR analyses for the palm oil and biodiesel obtained were performed using a Bruker AcendTM-400 spectrometer, which operates at 400.13 MHz for NMR ^{1}H and ^{13}C. Deuterated chloroform ($CDCl_3$) and TMS were used as a solvent and internal standard, respectively. ^{1}H (300 MHz) spectra were recorded with a 30° pulse duration, 1.0 s recycle delay, and eight scans. ^{13}C (75 MHz) spectra were recorded with a pulse duration of 30°, a recycle delay of 1.89 s, and 160 scans.

Results and analysis

Table 4 describes the nomenclature system used to assign names to the different starting substances and those synthesized in this investigation. Likewise, the process of obtaining each

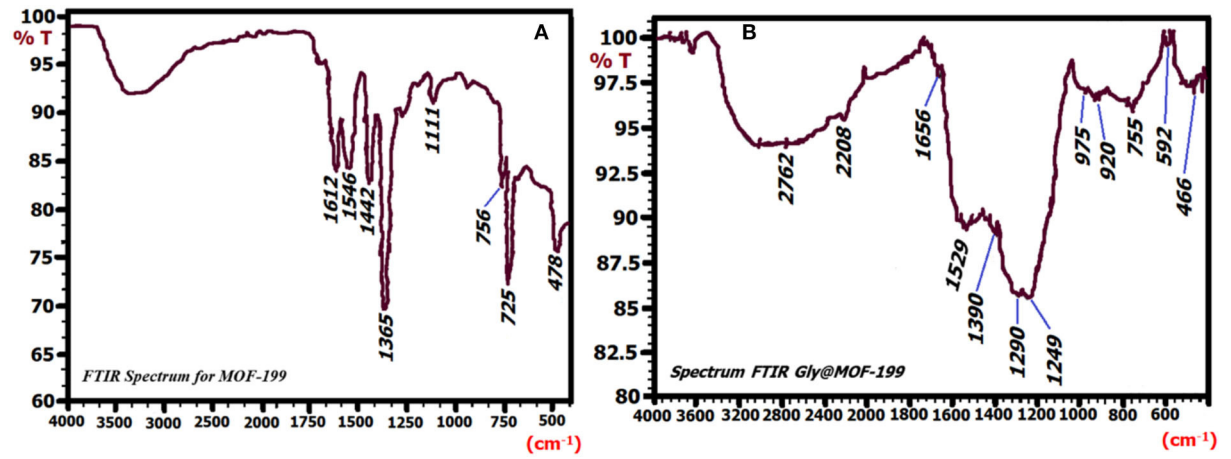

FIGURE 1
FTIR spectrum of: **(A)** MOF-199, **(B)** Gly@MOF-199.

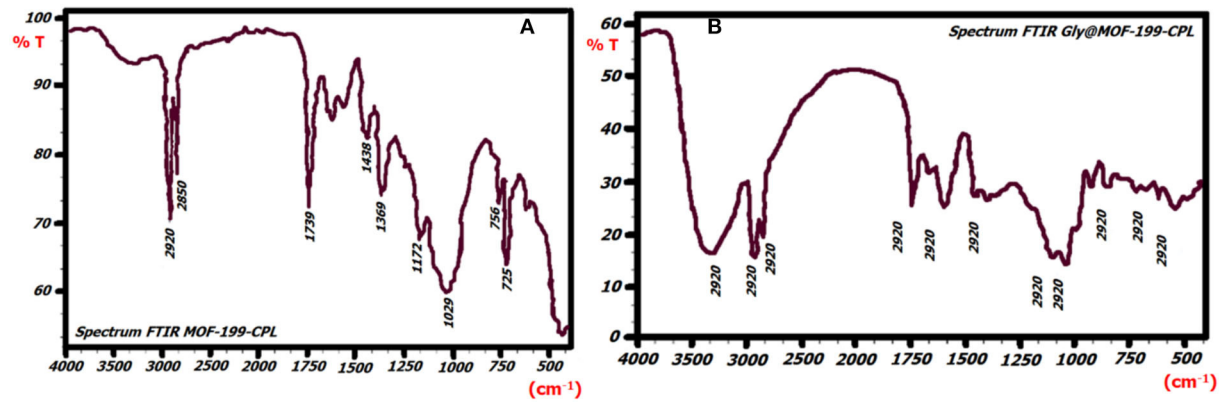

FIGURE 2
FTIR spectrum of: **(A)** MOF-199-PCL, **(B)** Gly@MOF-199-PCL.

of the biocatalysts and their corresponding samples based on biodiesel is summarized. Once the biodiesels were synthesized in the reactor, the two phases were separated. The biodiesels obtained were recovered and labeled using the prefix BIO.

Following, a comparative analysis of the spectra obtained by means of the FTIR, RAMAN, SEM-EDS, CG-MS, and NMR techniques is made.

TABLE 5 Conservation of vibration bands in the formation sequence of biomaterials.

Wave number (cm^{-1}) of catalytic materials			
MOF-199	**Gly@MOF-199**	**MOF-199-PCL**	**Gly@MOF-199-PCL**
478	466	725	543
725	592	756	621
756	756	1,029	856
1,111	920	1,772	925
1,365	975	1,369	1,047
1,442	1,249	1,438	1,111
1,546	1,290	1,739	1,406
1,612	1,529	2,850	1,460
3,475	1,656	2,920	1,597
			1,741
			2,852
			2,924

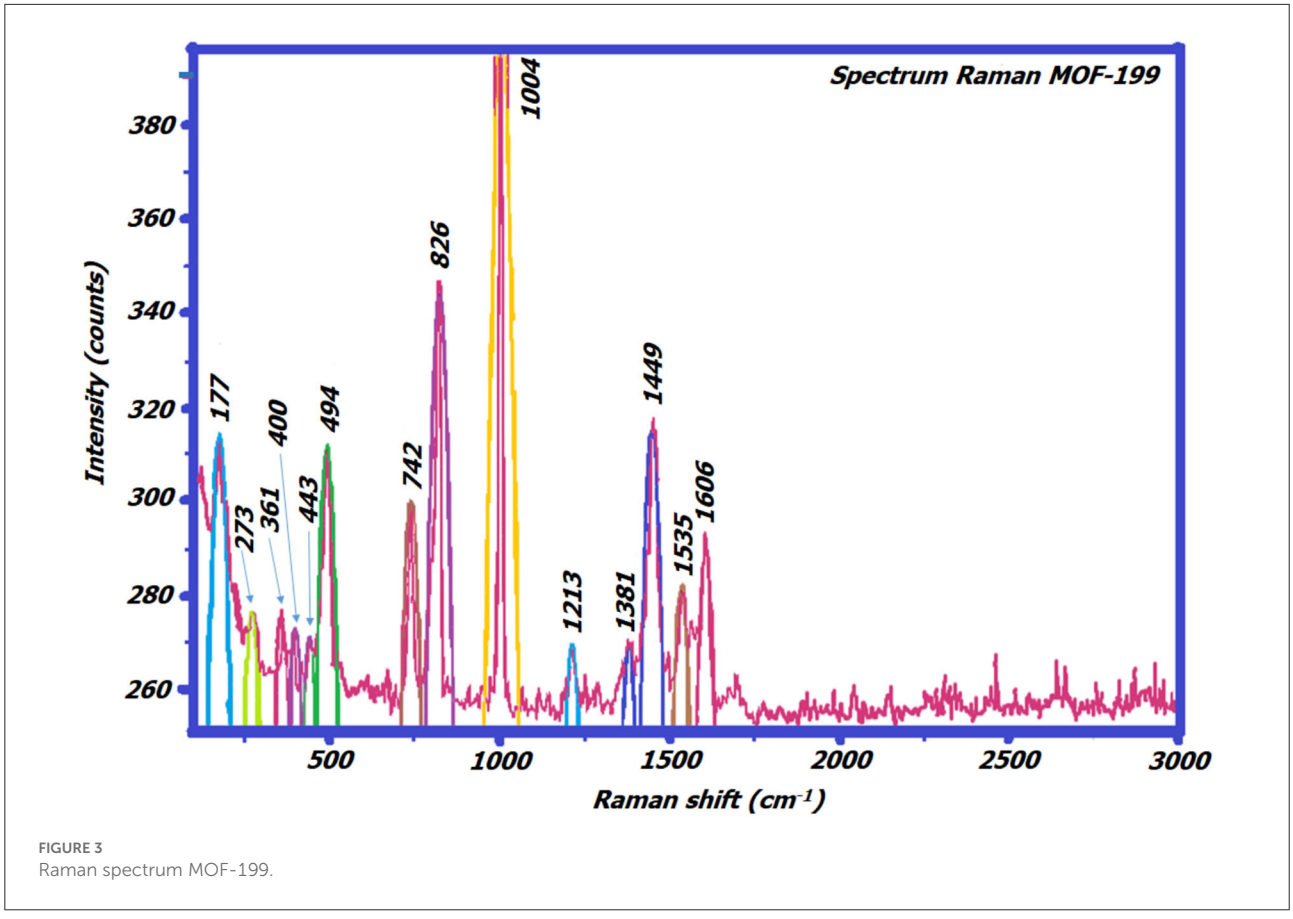

FIGURE 3
Raman spectrum MOF-199.

Preparation of catalytic materials: Analysis

Fourier transform infrared spectrophotometry, starting materials MOF-199, and Gly@MOF-199

Figure 1A shows the FTIR spectrum of MOF-199. The bands 1,546, 1,612, and 1,612 cm^{-1} correspond to the asymmetric stretching vibrations of the carboxylate groups of BTC and the bands 1,365 and 1,442 cm^{-1} correspond to the symmetric stretching vibrations of the carboxylate group of BTC, finally the bands 478, 725, 756, and 1,111 cm^{-1} correspond to the vibrations regarding the interaction of Cu^{2+} with the carboxylate groups, in agreement with Li et al. (2013).

Figure 1B shows the spectrum of Gly@MOF-199, where the displacement of the bands corresponding to the vibrations in terms of the interaction of Cu^{2+} with the carboxylate groups at lower wavenumbers (466, 592, and 756 cm^{-1}) is attributed to the temperature increase caused by pyrolysis in comparison to MOFF-199. The bands above 900 cm^{-1} possibly correspond to out-of-plane C–O–H bending vibrations (920 and 975 cm^{-1}); C–O–C stretching vibrations (1,249 and 1,290 cm^{-1}); symmetric and asymmetric stretching of carboxylate ligands in BTC (1,529, 1,529, and 1,656 cm^{-1}) (Chen et al., 2019); the bands corresponding to vibrations 2,208 and 2,762 cm^{-1} can be attributed to the interaction of C–C and C–O bonds by forming a carbonaceous and porous shell around the MOF structure, which provides protection. Stability allows the interaction of the MOF without suffering damage in relation to pressure or temperature in reactions mediated by this catalyst.

Fourier transform infrared spectrophotometry, MOF-199-PCL, and Gly@MOF-199-PCL biocatalysts

Figures 2A,B show the FTIR spectra of the biocatalysts; MOF-199-PCL and GlyMOF-199-PCL, some characteristic bands of MOF-199 are conserved in both spectra, and bands 725 and 756 cm^{-1} are present in both MOF-199 and MOF-1999-PCL, which indicates the conservation of the MOF-199 organo-metallic skeleton. Additionally, the presence of the 1,111 cm^{-1} band in both MOF-199 and Gly@MOF-199-PCL indicated the conservation of cooper with the carboxylate groups of the BTC after the modification of MOF-199.

The bands (2,850 and 2,920 cm^{-1}) present in MOF-199-PCL are conserved in Gly@MOF-199-PCL with a slight shift to a higher wave number (2,852 and 2,924 cm^{-1}), and interaction that was attributed to the anchoring of the carbonaceous shell to the MOF-199 structure through the formation of C–C and C–O bonds inherited from Gly@MOF-199. This same behavior is manifested with

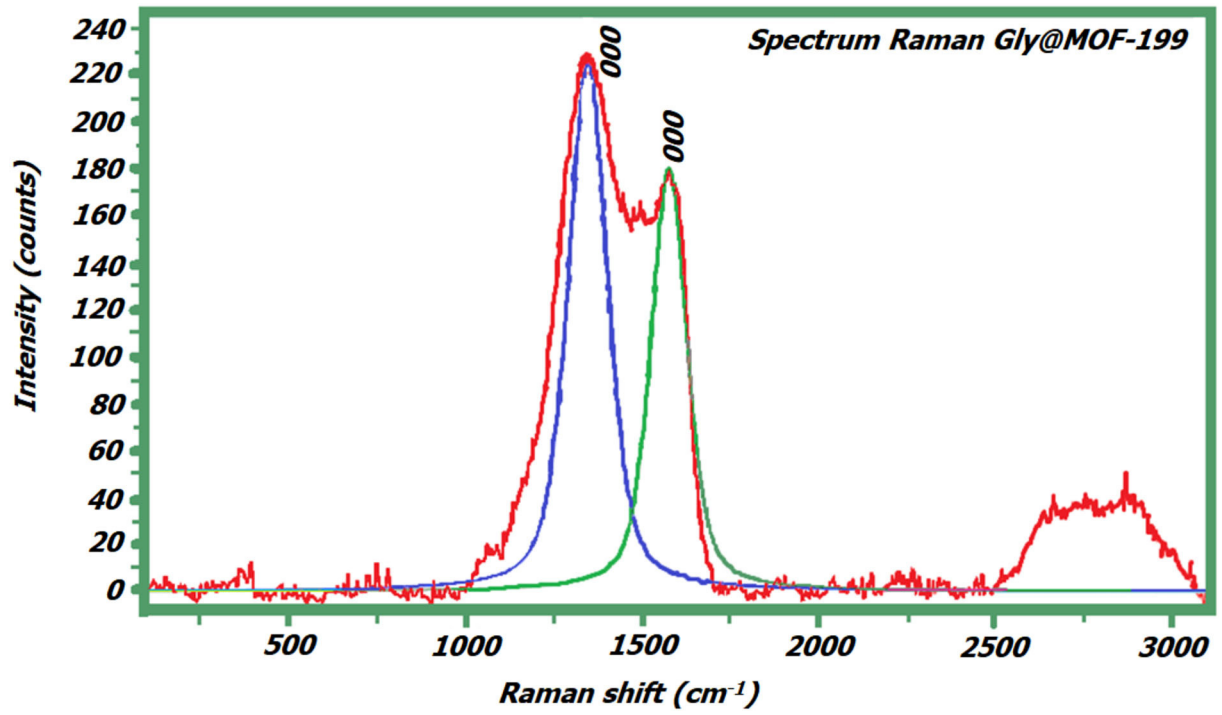

FIGURE 4
Raman spectrum Gly@MOF-199.

the band 920 and 925 cm^{-1} between Gly@MOF-199 and Gly@MOF-199-PCL, corroborating the conservation of the structure of MOF-199 and the formation of a carbonaceous core or network that wraps up. Table 5 illustrates the relationships between the bands of the four (4) catalytic materials.

The other bands in the MOF-199-PCL (1,029, 1,772, 1,369, 1,438, and 1,739 cm^{-1}) and in the Gly@MOF-199-PCL (543,

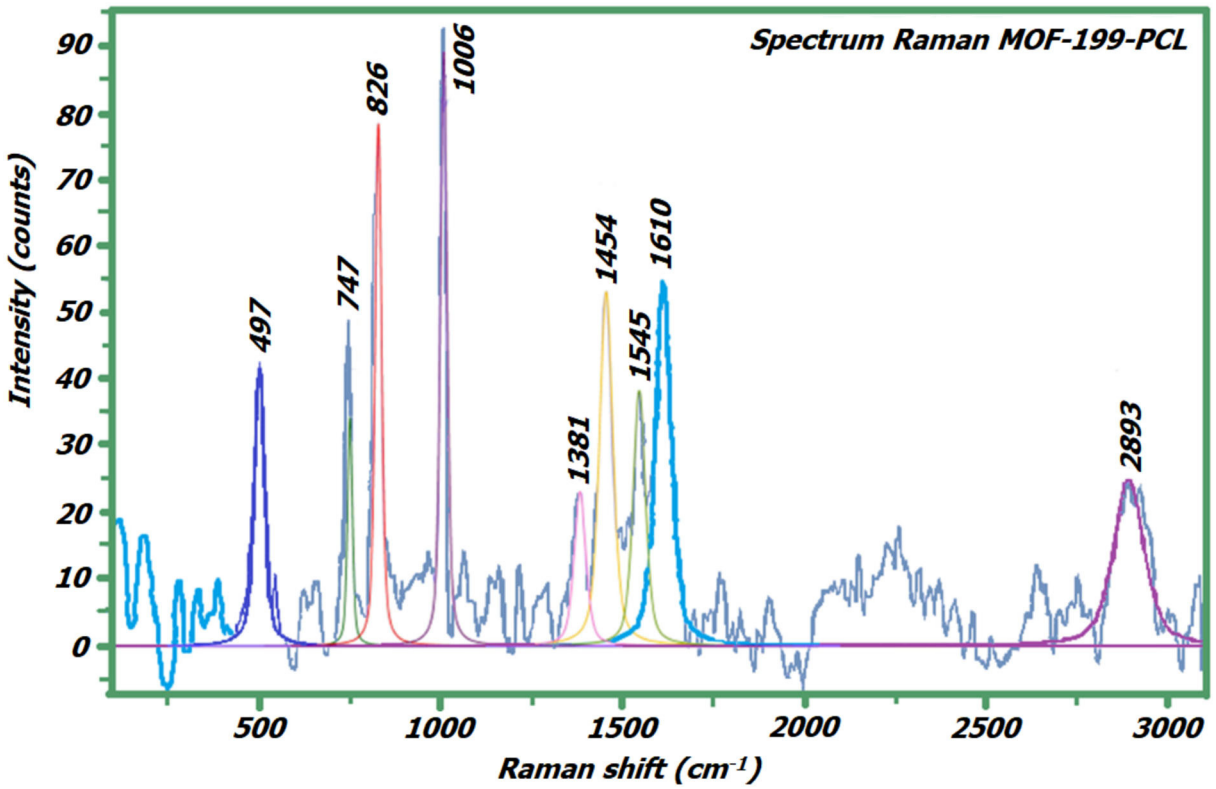

FIGURE 5
Raman spectrum MOF-199-PCL.

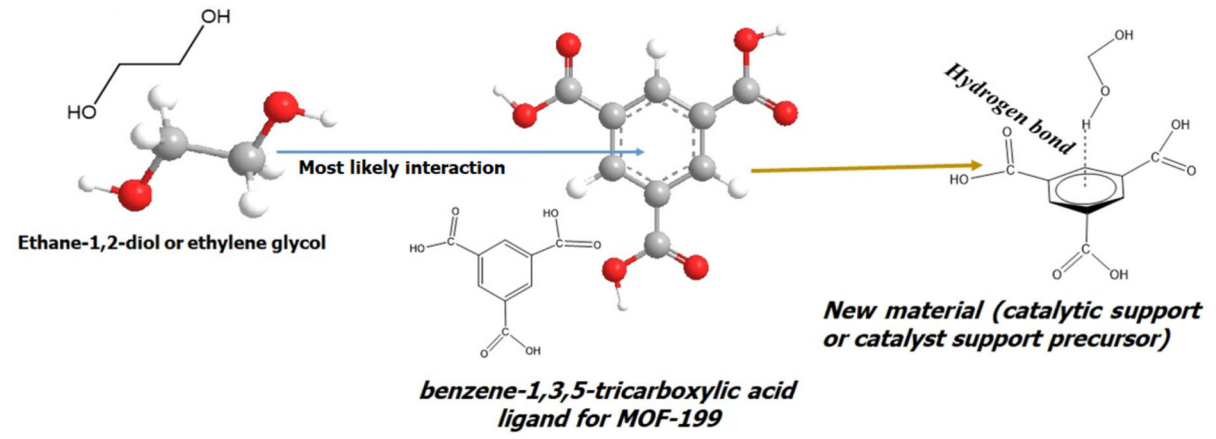

FIGURE 6
Formation pathway of the support or precursor MOF-199-ethylene glycol.

621, 856, 1,047, 1,406, 1,460, 1,597, and 1,741 cm^{-1}), possibly can be attributed to the iterations of the hydrophobic amino acids of lipase with the hydroxy and phenyl groups of the substrate. According to studies carried out by Lemke et al. (1997), it is known that the hydrophobic amino acids of lipases form substructures in the form of pockets, which facilitate interaction with the substrate by deforming when interacting with related groups present in the substrate. These pockets are more likely to attach to hydroxy, phenyl, phenoxymethyl, and phenoxymethyl groups than to other functional groups present on the substrate. MOF-199 has hydroxyl groups connected to the phenyl group (BTC units). Gly@MOF-199 retains the shape of these groups but is surrounded by a porous carbonaceous shell formed by ethylene glycol in the calcination process at 900°C. As MOF-199 has more exposed hydroxy groups connected to phenyl groups in relation to Gly@MOF-199, the interaction of *Pseudomonas cepacia* lipase with these groups is favored; however, the anchoring of lipase to the MOF surface-199 is limited by its large volume. In Table 5, an increase in the number of bands in Gly@MOF-199-PCL can be observed in relation to MOF-199-PCL, a fact that can be attributed to the increase in the interactions of the active sites of the lipase due to the increase in the pore size given by the formation of the carbonaceous shell around the structure in the form of an organo-metallic framework that remained after the thermal deprivation of MOF-199. That is, the new material takes the form of an organo-metallic framework [see section Morphological Analysis Semi-quantitative Chemical Composition (SEM-EDX)], despite the fact that MOF-199 decomposes with increasing temperature due to its thermal stability above 400°C (Tranchemontagne et al., 2008); however, the organo-metallic frameworks as a template transmit their morphology to the derivative (Dong et al., 2018) resulting from calcination at 900°C. The interaction of the lipase with the Gly@MOF-199 can be carried out by the pockets and the BTC units through the pores of the carbonaceous shell, which gives the lipase greater stability when anchored, compared to when it interacts directly with BTC units.

Raman spectroscopy, starting materials MOF-199 and Gly@-199

To determine the information on the effect of the modification of MOF-199 with ethylene glycol and immobilization of *Pseudomonas cepacia* lipase on the structure of the materials MOF-199 and Gly@MOF-199 (Figures 3, 4), these were characterized using Raman spectroscopy. For MOF-199, shift bands were observed at 177 and 494 cm^{-1} due

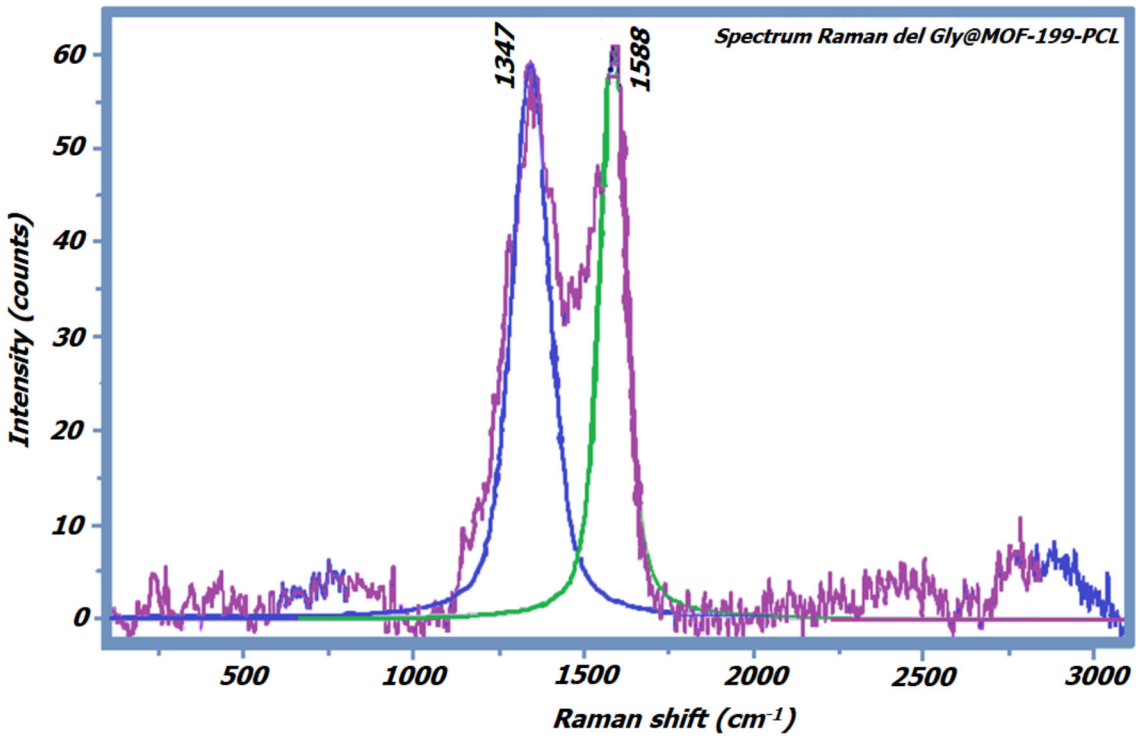

FIGURE 7
Raman spectrum Gly@MOF-199-PCL.

to Cu-O stretching (Dong et al., 2017). The peak at 1,449 and 1,449 cm^{-1} corresponds to the vibrations of the functional groups COO^{-} (Deshmukh et al., 2018). The peaks at 742 and 826 cm^{-1} correspond to out-of-plane ring bending vibrations of C=C and out-of-plane C–H bending on the phenyl ring of the BTC ligand.

The peaks at 1,004 and 1,606 cm^{-1} correspond to the C=C vibrational band in the benzene ring. The 1,449 cm^{-1} peak corresponds to COO–(carboxylate) symmetric stretching vibrations and the 1,535 cm^{-1} peak corresponds to stretching vibrations (Dong et al., 2017). The foregoing confirms that the analyzed material, indeed, corresponds to MOF-199. The spectrum of Gly@MOF-199 is completely different, showing that the impregnation with ethylene glycol and subsequent calcination effectively modified MOF-199 structurally. The characteristic bands for this new material are: 1,348 and 1,577 cm^{-1}. The first band corresponds to the C–C tension (Guerrini, 2009) of the porous carbonaceous material formed by modifying MOF-199 in the presence of ethylene glycol; the second band corresponds to the vibrations regarding the interaction of the carbons of the structure in the form of MOFs anchored to the shell or external porous carbonaceous network, through the Cu^{2+} ions.

TABLE 6 Vibrational bands of the starting materials and biocatalysts, determined by Raman spectroscopy.

Wave number (cm^{-1}) of catalytic materials			
MOF-199	**Gly@MOF-199-PCL**	**MOF-199-PCL**	**Gly@MOF-199-PCL**
177	1,348	497	1,508
273	1,577	747	1,847
361		826	
400		1,006	
443		1,381	
494		1,454	
742		1,545	
826		1,610	
1,004			
1,213			
1,381			
1,449			
1,535			
1,606			

Raman spectroscopy, MOF-199-PCL, and Gly@MOF-199-PCL biocatalysts

Figure 5 shows the Raman spectrum of the MOF-199-PCL biocatalyst, in which the bands 497, 747, 826, 1,006, and 1,381 cm^{-1} are distinguished, which are characteristic signals of MOF-199, with a slight shift toward higher band numbers from vibrations 494 and 742 cm^{-1} to vibrations 497 and 747 cm^{-1}. The bands 1,454, 1,545, and 1,610 cm^{-1} are attributed to the different interactions of the terminals of the hydrophobic amino acids with the phenyl and hydroxyl groups of the SBUs of the MOF structure. These groups present on the supports constitute anchorage sites for the *Pseudomonas cepacia* lipase. Hydroxyl groups is more exposed because the anchoring of ethylene glycol occurs through the formation of hydrogen bonds between the hydrogens of the hydroxyl groups of ethylene glycol with 1,3,5-benzene tricarboxylic acid, which acts as a ligand of MOF-199, this ligand presents resonance through the phenyl ring, the high density of this electronic cloud attracts hydrogen deficient electrons from one of the extreme hydroxyl groups of ethylene glycol, facilitating the formation of hydrogen bonds (see Figure 6), this iteration is possible because the medium

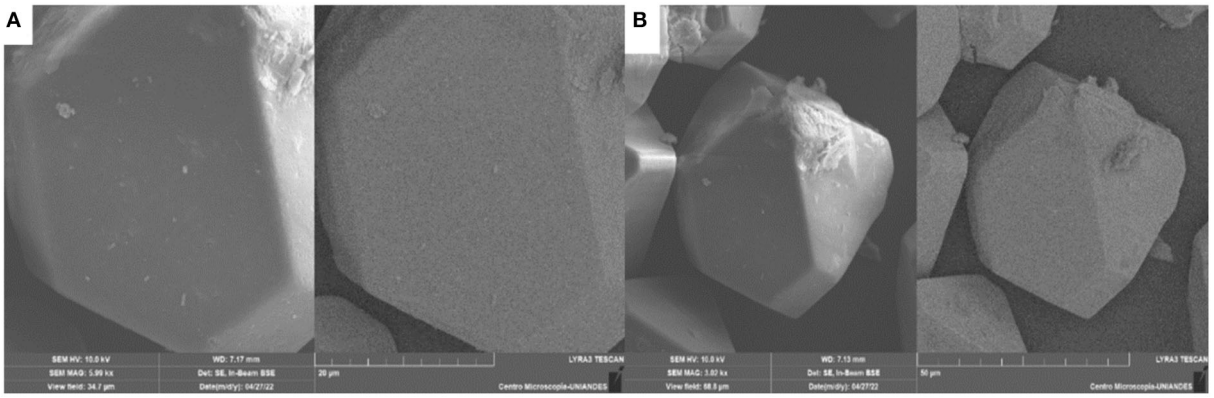

FIGURE 8
SEM-EDS microphotographs of MOF-199: **(A)** magnification at 3.02kx, **(B)** magnification at 5.99kx.

maintains a pH of 7 and the pK_a of ethylene glycol is 14.4 (Woolley et al., 1972). Ethylene glycol binds to the MOF-199 structure by one of the hydroxyl groups at one end, leaving the hydroxyl groups at the other end exposed to the action of the hydrophobic amino acids of the *Pseudomonas cepacia* lipase, which have preferences for groups with high electron density (Lemke et al., 1997).

Figure 7 shows the Raman spectrum of Gly@MOF-199-PCL, in which they present two vibrational bands (1,508 and 1,847 cm^{-1}), which are attributed to two types of interactions. The first interactions are carried out between the terminals of the hydrophobic amino acids with the phenyl and hydroxy groups of the SBUs of the MOF structure through the pores of the porous carbonaceous material that surrounds the MOF-type structure, which in turn allows for greater stability, due to immobilization by the formation of covalent bonds and anchoring of the lipase to the pore (double anchoring), thus the binding of the substrate lipase is much stronger the degrees of freedom decrease in relation to the given interaction between lipase and the hydroxyl groups for the

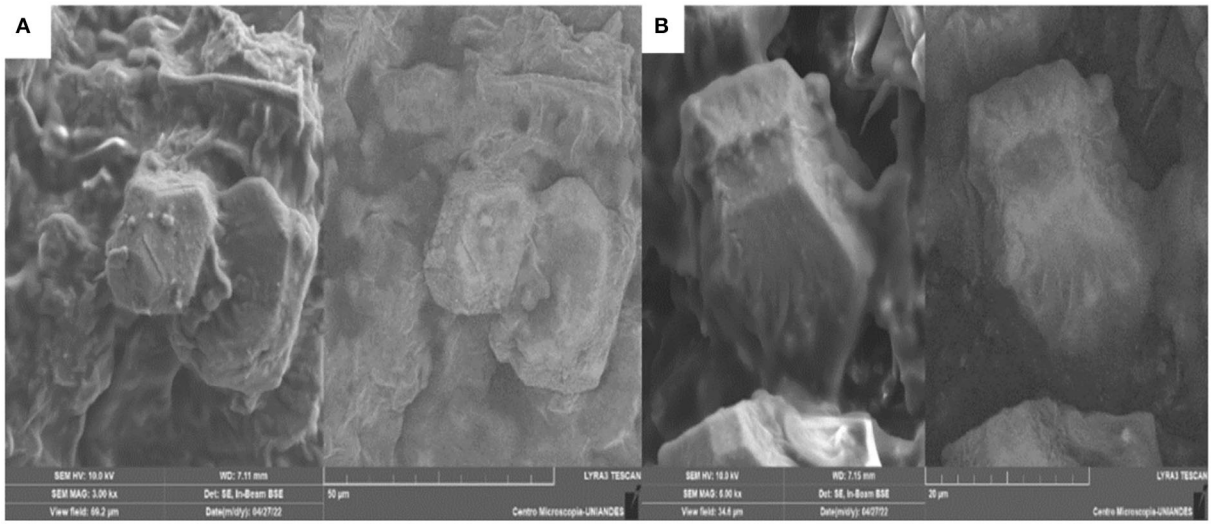

FIGURE 9
SEM-EDS microphotographs of Gly@MOF-199: **(A)** magnification at 3.00kx, **(B)** magnification at 6.00kx.

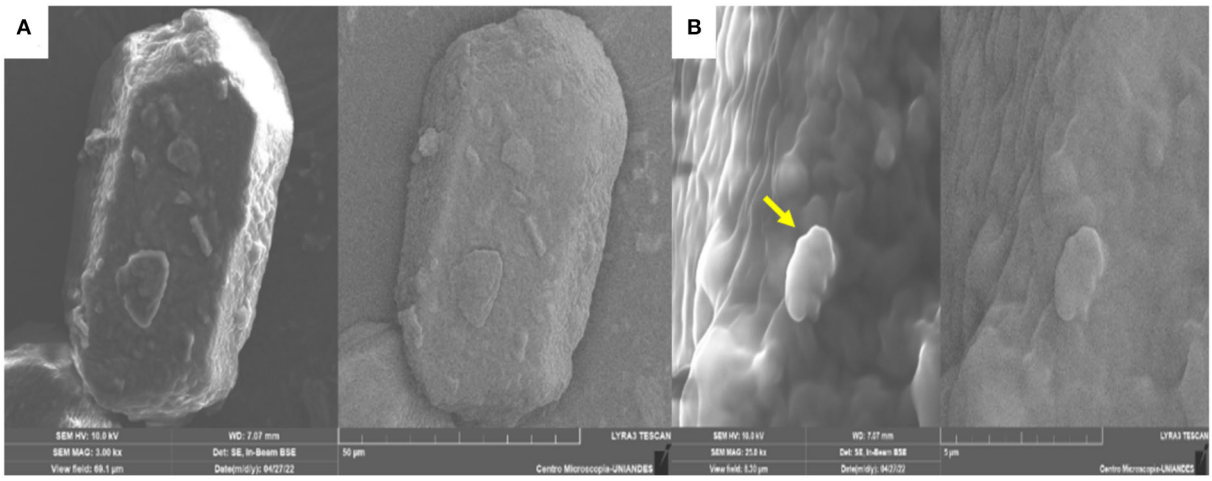

FIGURE 10
SEM-EDS microphotographs of MOF-199-PCL: **(A)** magnification at 3.02kx, **(B)** magnification at 25.00kx *Pseudomonas cepacia* lipase indicated with the yellow arrow.

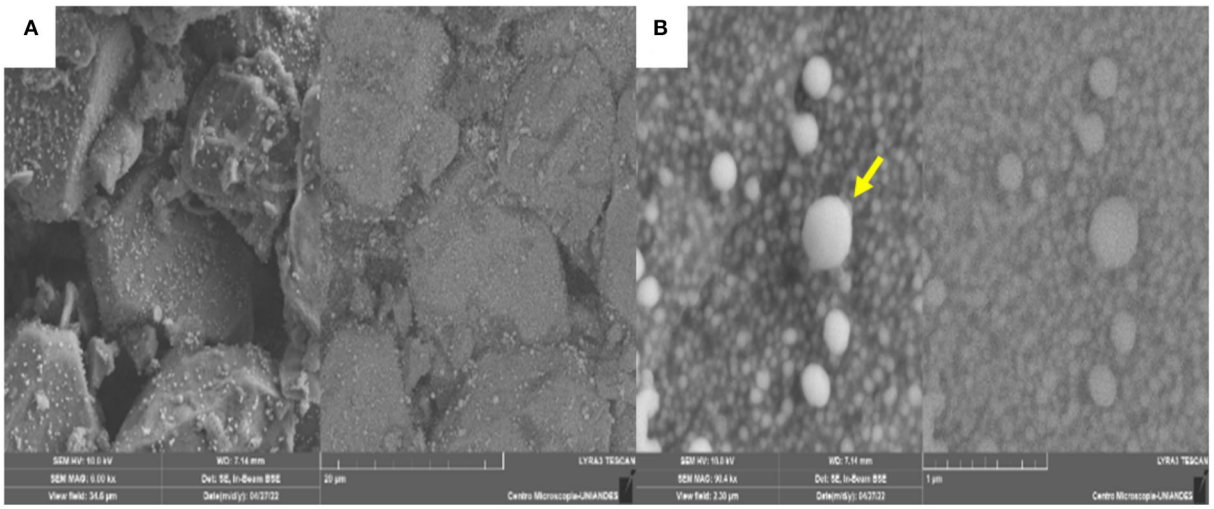

FIGURE 11
SEM-EDS microphotographs of GlyqMOF-199-PCL: **(A)** magnification at 6.00kx, **(B)** magnification at 90.4kx. Pseudomonas cepacia lipase indicated with the yellow arrow.

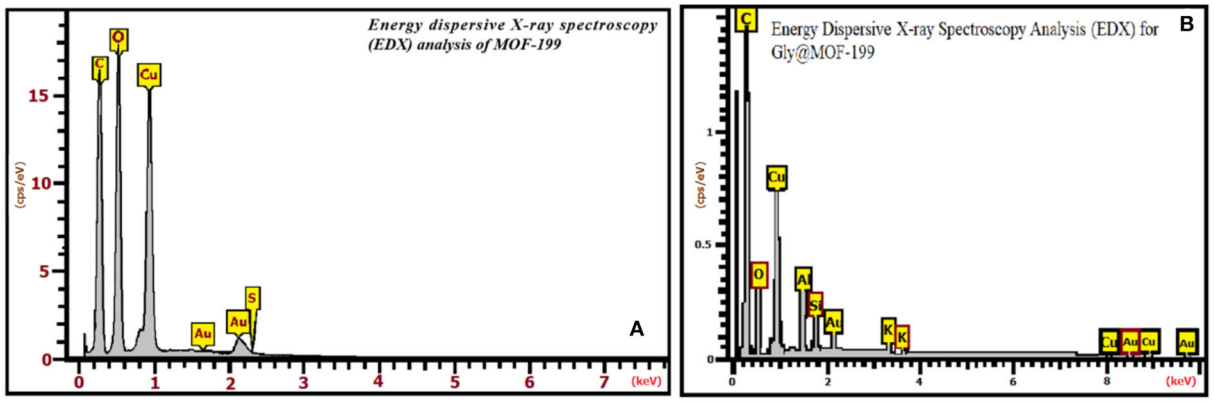

FIGURE 12
Energy dispersive X-ray spectroscopy (EDX) analysis: **(A)** MOF-199, **(B)** Gly@MOF-199.

case of the formation of the biocatalyst MOF-199-PCL. The second interaction occurs directly between the hydrophobic fractions of the amino acids of the *Pseudomonas cepacia* lipase with the copper that was immersed or on the surface of the shell or carbonaceous network in the modified MOF, as reported by Díaz-Duran and Roncaroli (2021) for cobalt. These surface copper atoms are subject to carbon atoms from the thermal decomposition of the phenyl groups when calcined at 900°C. The carbonaceous shell formed by the thermal decomposition of ethylene glycol prevents the Cu atoms from fully migrating to the surface of the y acquire an umbrella-shaped orientation looking toward the interior of the cavity formed by the carbonaceous material. Table 6 shows a summary of the vibrational bands of the catalytic materials determined by Raman spectroscopy.

Morphological analysis semi-quantitative chemical composition (SEM-EDX)

Starting materials MOF-199 and Gly@MOF-199 and biocatalysts MOF-199-PCL and GlyMOF-199-PCL

The SEM-EDS images in Figures 8–11 clearly show the conservation of the morphology and the crystalline nature of pure MOF-199, which evidences the transmission of the MOF structure to its derivatives. The SEM-EDS image in Figures 8A,B,

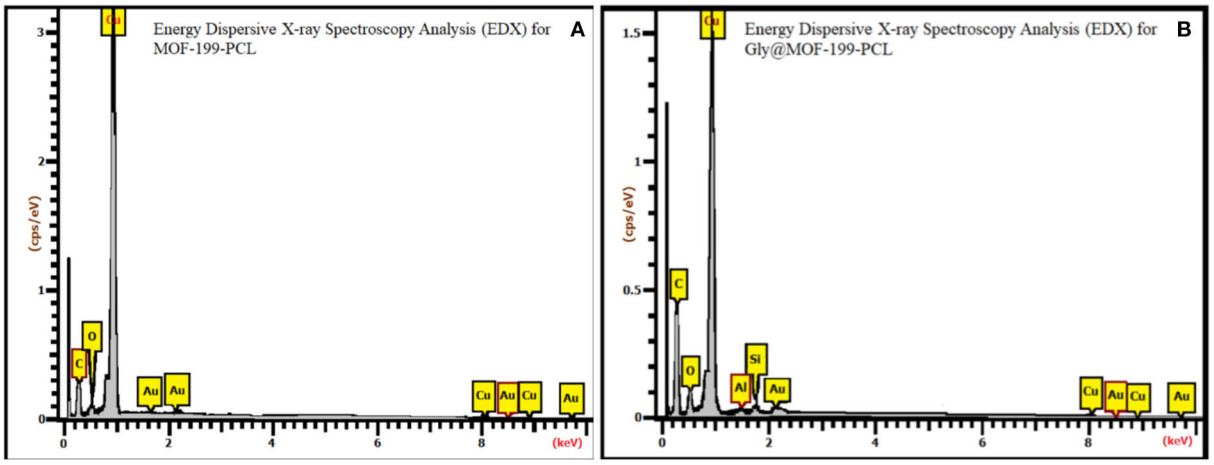

FIGURE 13
Energy dispersive X-ray spectroscopy (EDX) analysis: **(A)** MOF-199-PCL, **(B)** GlyMOF-199-PCL.

TABLE 7 EDX elemental analysis data of Gly@MOF-199, MOF-199-PCL, synthesized Gly@MOF-199-PCL, and MOF-199.

	MOF-199		Gly@MOF-199		MOF-199-PCL		Gly@MOF-199-PCL	
Element	**% weight**	**% atomic**	**% weight**	**% atomic**	**% weight**	**% atomic**	**% weight**	**% atomic**
C	43.45	60.91	35.41	70.05	70.79	82.41	23.96	60.77
O	30.57	32.17	4.74	7.04	15.97	13.96	1.95	3.72
Na	0	0	0	0	0.35	0.21	0	0
S	0.14	0.07	0	0	0	0	0	0
Al	0	0	0.40	0.35	0	0	0	0
Si	0	0	0.36	0.11	0.45	0.23	0	0
P	0	0	0	0	1.13	0.51	0	0
K	0	0	0.67	0.17	1.42	0.51	0	0
Cu	25.84	6.85	58.42	21.85	9.46	2.08	74.09	35.51
Total	100	100	100	100	100	100	100	100

9A,B shows the morphological changes undergone by MOF-199 when thermally modified in the presence of ethylene glycol, at different magnifications, observing their changes. The calcination caused an increase in the pore volume, which allows the lipase to anchor more easily. The SEM-EDS images in Figures 10, 11 clearly show the presence of *Pseudomonas cepacia lipase* immobilized on the surface of MOF-100 and Gly@MOF-199, respectively. It can be seen in the microphotograph of MOF-199-PCL (see Figures 10A,B) that lipase does not present a homogeneous distribution on the surface of MOF-199, while Figures 11A,B show a greater distribution of lipase, the effect of increased area exposed by increasing the pore size.

Figures 12, 13 show energy dispersive X-ray spectroscopy (EDX) images for the pure MOF-199, Gly@MOF-199, MOF-199-PCL, and Gly@MOF-199-PCL samples. All spectra clearly show the presence of the element copper (Cu), both for pure MOF-199 (Figure 12A), as well as for sample Gly@MOF-199 (see Figure 12B). The presence of copper confirms the preservation of the structure and morphology of the support. The conservation of structure and morphology in the derivatives MOF-199-PCL, Gly@MOF-199, and Gly@MOF-199-PCL (see Figures 13A,B) indicates that MOF-199 not only behaves as a precursor of the new materials but also as a structure template when used for the formation of catalytic supports for the immobilization of lipase from *Pseudomonas lipase*. Table 7 shows the elemental composition of the four (4) catalyst materials.

The data regarding the atomic concentration of Cu in each of the analyzed materials confirm the synthesis of Gly@MOF-199, MOF-199-PCL, and Gly@MOF-199-PCL and additionally corroborates the conservation of BTC units. The increase in the percentage of Cu (58.42 and 74.09) in the Gly@MOF-199

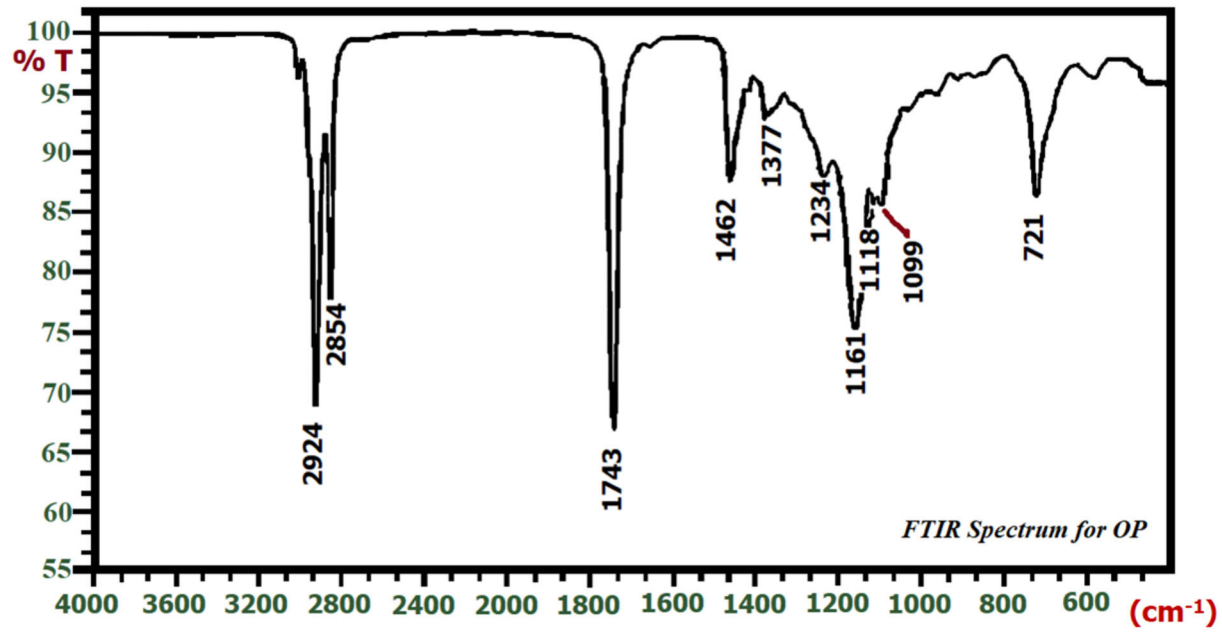

FIGURE 14
FTIR spectrum of commercial palm oil OP.

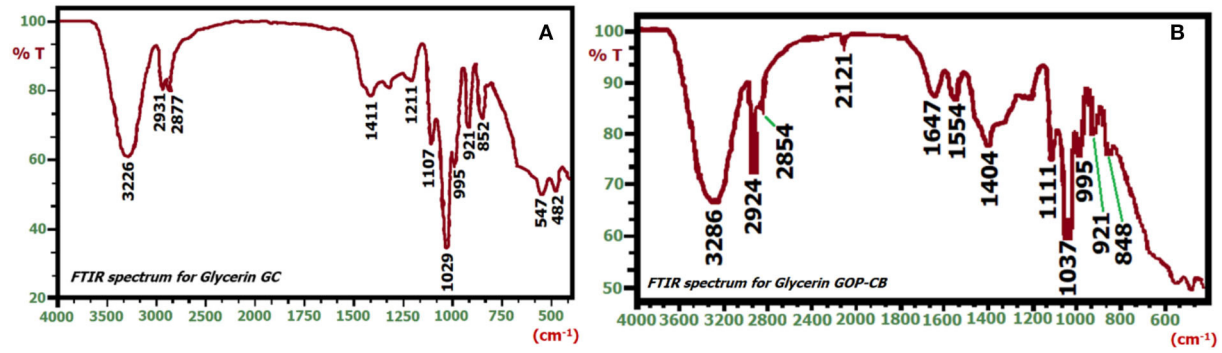

FIGURE 15
Comparison of FTIR spectra of glycerin: **(A)** commercial glycerin GC, **(B)** glycerin synthesized by basic catalysis GOP-CB.

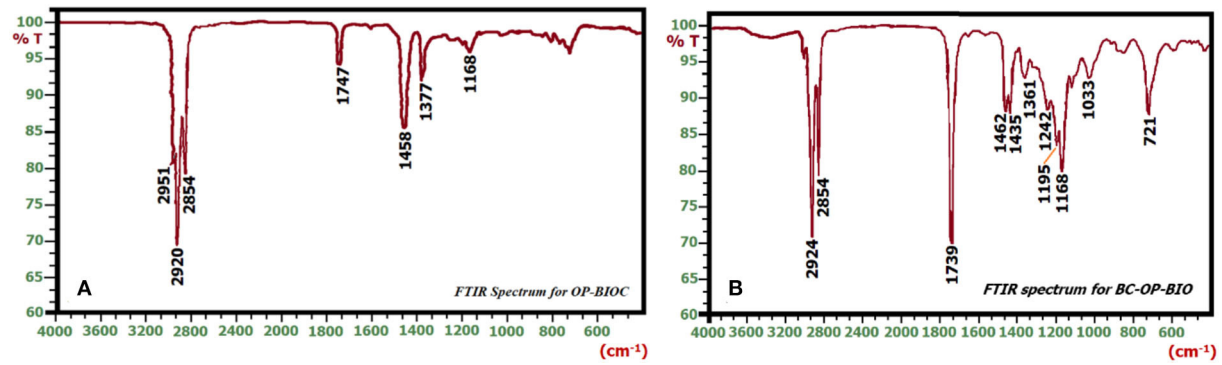

FIGURE 16
Comparison between the FTIR spectra: **(A)** BIOC commercial biodiesel, **(B)** biodiesel synthesized by basic catalysis BC-OP-BIO.

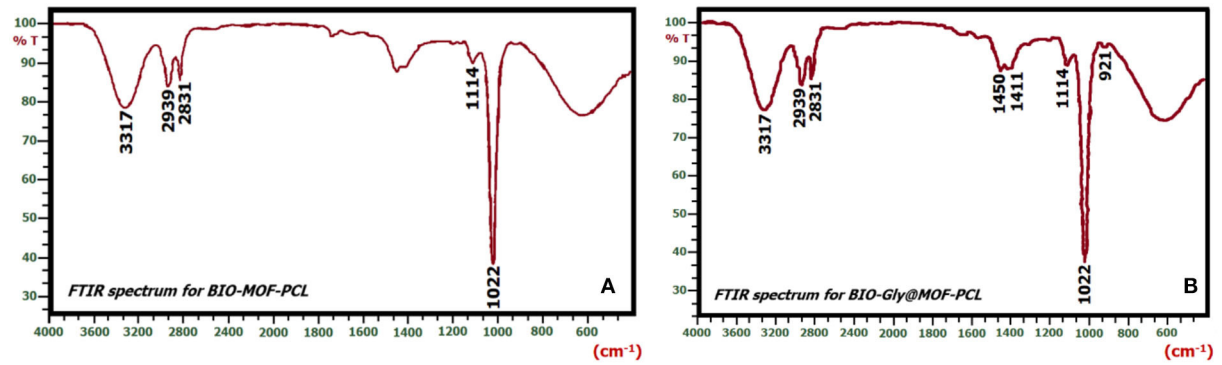

FIGURE 17
Synthesized biodiesel comparison: **(A)** BIO-MOF-199-PCL biodiesel, synthesized from the MOF-PCL biomaterial, **(B)** BIO-Gly@MOF-199-PCL biodiesel synthesized from the Gly@MOF-199 bio-catalyst.

TABLE 8 Similarity of vibration bands in the different synthesized biofuels.

Start-up	Comparatives			Biodiesel		
OP	OP-BIOC	CB-OP-BIO	GC	GOB-OP	BIO-MOF-199-PCL	BIO-GlyMOF-199-PCL
721	1,168	721	482	848	1022	921
1,099	1,377	1,033	547	921	1,114	1,022
1,118	1,458	1,168	852	995	1,411	1,114
1,161	1,747	1,195	921	1,037	1,450	1,411
1,234	2,854	1,242	995	1,111	2,831	1,450
1,377	2,920	1,361	1,029	1,404	2,939	2,831
1,462	2,951	1,435	1,107	1,554	3,317	2,939
1,743		1,462	1,211	1,647		3,317
2,854		1,739	1,411	2,121		
2,924		2,854	2,877	2,854		
		2,924	2,931	2,924		
			3,286	3,286		

and Gly@MOF-199-PCL materials, respectively, is attributed to the loss of mass due to the volatilization of oxygen during calcination at 900°C.

Biofuel production: Analysis

Fourier transform infrared spectrophotometry

Figures 14–17 show the FTIRs: of the OP starting material (see Figure 14); glycerin commercial GC and GOP-CB (see Figures 15A,B); comparisons between FTIR spectra are also presented: (A) Commercial biodiesel BIOC; (B) biodiesel synthesized by basic catalysis BC-OP-BIOC (see Figures 16A,B) and biodiesel synthesized by basic catalysis BC-OP-BIO and biofuels BIO-MOF-199-PCL, and BIO-Gly@MOF-199-PCL (see Figures 17A,B).

Table 8 shows all the results, using the FTIR technique, which has been assigned to vibrational bands for each of the biofuels synthesized by biocatalysts: the starting oils for transesterification; the biodiesel synthesized by basic catalysis (here we will call it "comparative"), and the biodiesel synthesized using the biocatalyst. This table shows that the 1,168 cm^{-1} band is present in both OP-BIOC and BC-OP-BIO, which indicates that these bands are characteristics of biodiesel. In this context, it is found that the same bands are present in the biofuels BIO-MOF-199-PCL and BIO-Gly@MOF-199-PCL (see Figures 17A,B), so it can be concluded that the liquid obtained using biocatalysts (with the biocatalyst synthesized in this research) with commercial palm oil is biodiesel. BIO-Gly@MOF-199-PCL differs from BIO-MOF-199-PCL because it presents the 921 cm^{-1} band, which is compared with commercial glycerin GC, which can be explained in two ways: (1) BIO-Gly@MOF-199-PCL has the presence of glycerin in

small amounts and (2) 1,3-propanetriol is part of the FAME structure in the form of mono or diacylglyceride attached to a methyl group through carbonyl groups, as reported (Jaecker-Voirol et al., 2008).

The BIO-MOF-199-PCL and BIO-Gly@MOF-199-PCL biocatalysts do not bear close similarities with the comparative biodiesels (OP-BIOC and BC-OP-BIO), but they do present two vibrational bands 2,939 and 3,137 cm^{-1} slightly shifted to higher wavenumbers in relation to the 2,920 and 2,951 cm^{-1} bands present in OP-BIOC. In addition, these two biofuels are very similar to each other since they share seven (7) bands: 1,022, 1,114, 1,411, 1,450, 2,831, 2,939, and 3,317 cm^{-1}, which are distinctive characteristics of this new biodiesel and in turn a consequence of transesterification to form two new biocatalysts (MOF-199.PCL and Gly@MOF-PCL). The only difference between these two biocatalysts is the presence of the 921 cm^{-1} band in the BIO-Gly@MOF-PCL, which is attributed to the GC glycerin fraction that was not

TABLE 9 GC-MS chemical composition of comparative biodiesels and synthesized biodiesels.

Assigned compound	%Área				Molecular formula
	OP-BIOC	CB-OP-BIO	BIO-MOF-199-PCL	BIO-Gly@MOF-199-PCL	
Methyl palmitate (**1**)	25.84	36.84	26.90	29.12	$C_{17}H_{34}O_2$
Methyl stearate (**2**)	5.24	0	5.13	4.98	$C_{19}H_{38}O_2$
Methyl oleate (**3**)	35.42	31.91	35.94	37.17	$C_{19}H_{36}O_2$
Methyl linoleate (**4**)	27.39	6.73	26.56	23.41	$C_{19}H_{34}O_2$
Methyl eicosatrienoate (**5**)	2.95	0	2.53	0	$C_{21}H_{36}O_2$

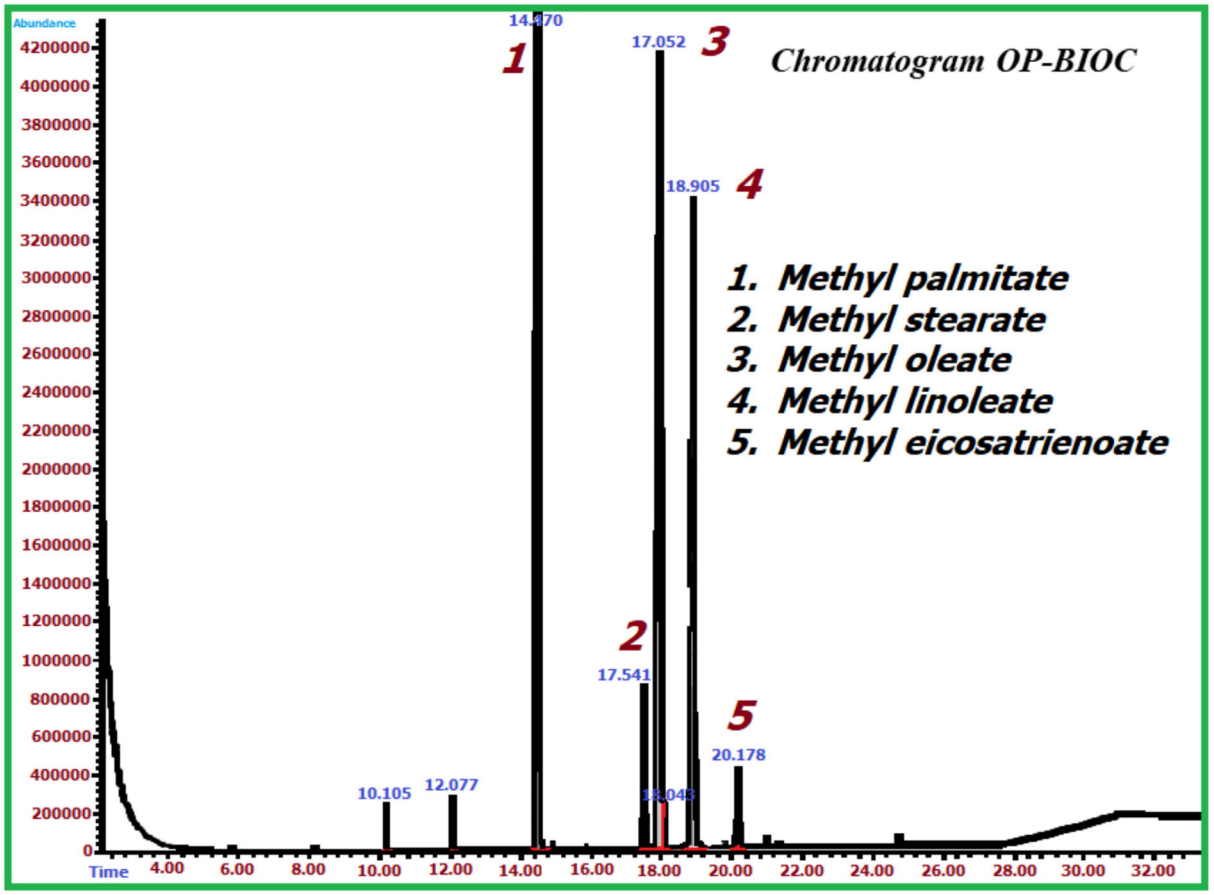

FIGURE 18
OP-BIOC commercial biodiesel chromatogram.

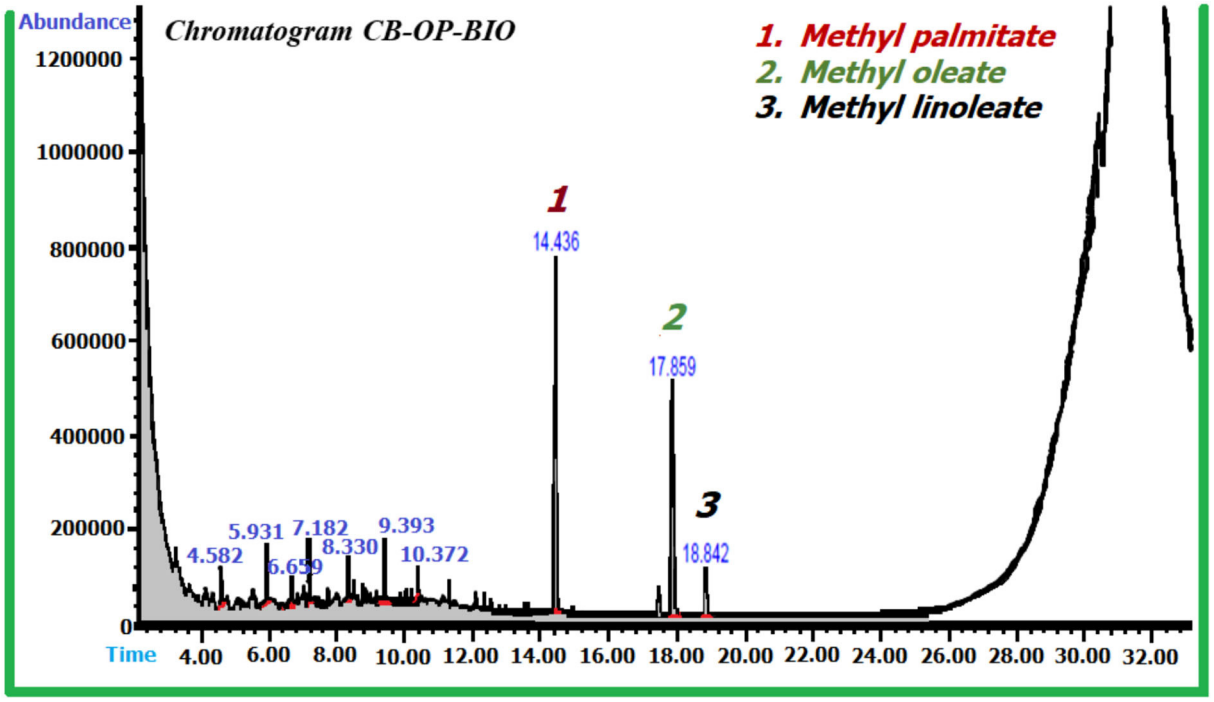

FIGURE 19
CB-OP-BIO biodiesel chromatogram synthesized from base catalysis.

completely transformed by the biocatalyst, that is, a partial transesterification of glycerin by the biocatalyst Gly@MOF-PCL or it can be attributed to the presence of traces of glycerin remaining due to poor phase separation; however, in the fractions separated when synthesizing biodiesel by biocatalysis it has not been possible to detect the presence of glycerin as if it occurs in the transesterification of palm oil by base catalysis (see Figure 16B). The presence of the 1,450 cm^{-1} band in BIO-MOF-PCL and BIO-Gly@MOF-PCL is due to a slight shift toward a higher wavenumber compared to the 1,458 cm^{-1} band present in OP-BIOC, a fact which corroborates the synthesis of biodiesel.

It is noteworthy that the MOF-199-PCL biocatalyst converted palm oil (OP), as the starting raw material, into biodiesel without the presence of glycerin being noted in the FTIR spectrum. With Gly@MOF-199.PCL, it can be inferred as a first alternative that this catalyst promoted the formation of glycerin that became part of the biological diesel mixture known as Ecodiesel (Calero et al., 2020), as a second alternative it can be inferred that glycerin remains embedded as R chain in FAME. The presence of the 2,854 cm^{-1} band in all the synthesized biofuels is not determined to determine if these substances correspond to biodiesel, because this vibrational band is also present in the comparative biofuels (OP-BIOC and BIO-AP-CB).

Gas chromatography coupled to masses

Chromatographic identification

The chromatograms of biodiesel, commercial OP-BIOC, and basic catalysis CB-OP-BIO show that these biofuels are fatty acid esters mixtures. They have the following FAMES in common: methyl palmitate, oleate, and linoleate. The most abundant FAME in OP-BIOC is methyl oleate, while the most abundant in CB-OP-BIO is methyl palmitate (see Table 9). The significant difference between these two biodiesels lies in the fact that OP-BIOC commercial biodiesel contains methyl stearate and eicosatrienoate (see Figures 18, 19). The chromatograms of the biodiesels BIO-MOF-199-PCL and BIO-Gly@MOF-199-PCL (see Figures 20, 21) present percentages in an area similar to OP-BIOC for the esters: palmitate, oleate, stearate and linoleate of methyl, with methyl oleate being the most abundant FAME in the three biofuels.

The FAMES concentrations in BIO-Gly@MOF-199-PCL and BIO-Gly@MOF-199-PCL are similar, which implies that the performance of the Gly@MOF-199-PCL biocatalyst remained constant, a behavior that it can be attributed to the stability of the *Pseudomonas cepacia* lipase anchoring on the surface of the supports. Additionally, it is verified that the modification of MOF-199 in the presence of ethylene glycol provided greater anchorage of the active sites, thus allowing a better distribution and immobilization of the *Pseudomonas cepacia* lipase; however, this double anchorage brings with it a loss

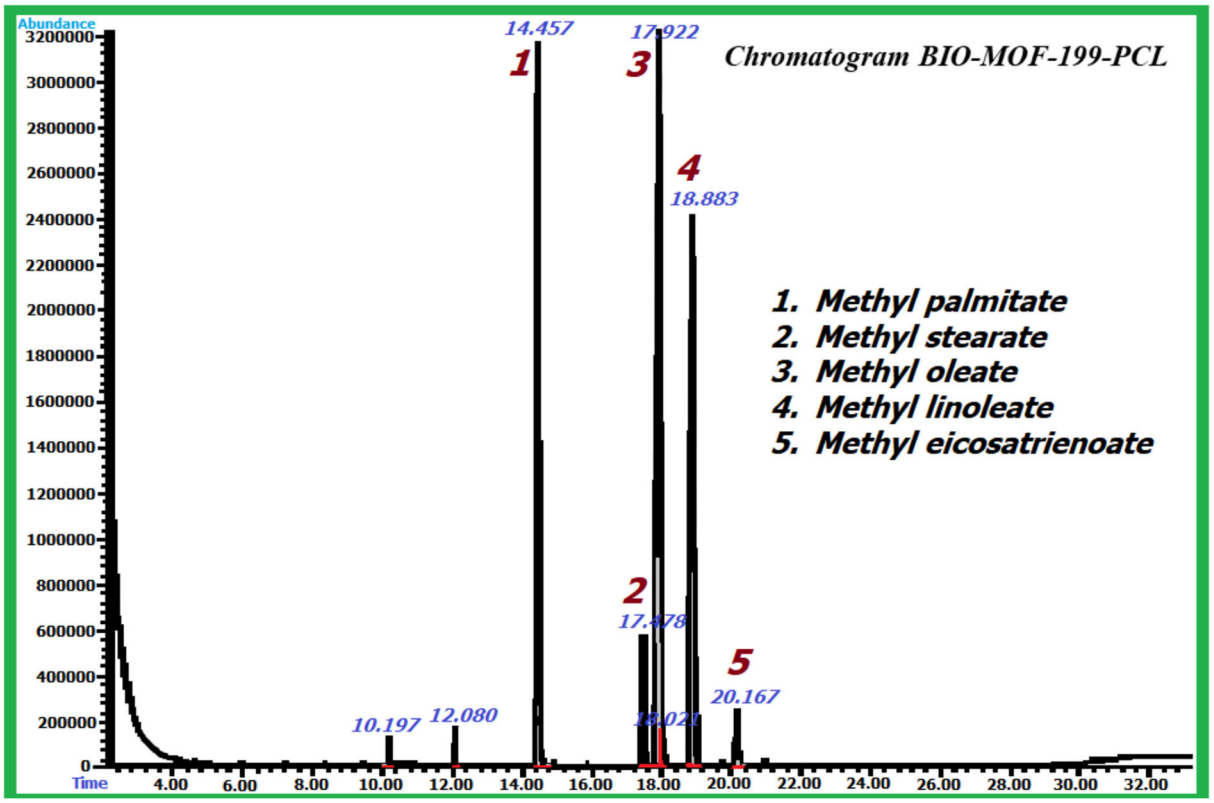

FIGURE 20
BIO-MOF-199-PCL biodiesel chromatogram synthesized by biocatalysis.

of the degrees of freedom; therefore, the anchored lipase has less capacity to transesterify and hence the presence of paraffin, such as tetradecane, pentadecane, hexadecane, and heptadecane, in small percentages as shown in Table 11. This biofuel results from the mixture of FAMEs with aliphatic hydrocarbons type of high molecular weight paraffin, also known as green diesel (Chaudhari et al., 2021). The formation of FAMES fatty acid esters is indicative of the occurrence of transesterification reactions mediated by the biocatalysts MOF-199.PCL and Gly@MOF-199-PCL, as well as the absence of free fatty acids (see Table 10) in the synthesized biodiesel are indicative of the occurrence of esterification reactions. In this scenario, the implications of this process for the production of biodiesel from the biocatalysts MOF-199-PCL and Gly@MOF-199-PCL derived from the immobilization of *Pseudomonas cepacia* lipase on MOF-199 support modified by two alternative synthesis routes represents a new simultaneous process for transesterification/esterification reactions with the added value of detecting glycerin traits in the produced fractions.

Mass analysis

To corroborate the identification of fatty acids, mass spectroscopy was applied. Only the OP-BIOC, BIO-MOF-199-PCL, and BIO-Gly@MOF-199-PCL mass spectra are described (see Table 9). The spectra obtained for each fatty acid were compared with the database (SOFWARE Xcalibur).

Table 10 shows that the MOF-199-PCL and Gly@MOF-199-PCL biocatalysts convert free fatty acids into FAMEs, a fact that is corroborated by the non-presence of these compounds in the chromatograms of these biocatalysts. This finding is important because it implies that these new catalytic materials perform simultaneous transesterification and esterification reactions. Table 11 shows the presence of paraffin-type compounds in the biofuel with BIO-Gly@MOF-199-PCL formulation, which implies that the substance synthesized from this catalyst corresponds to a liquid biofuel called green diesel.

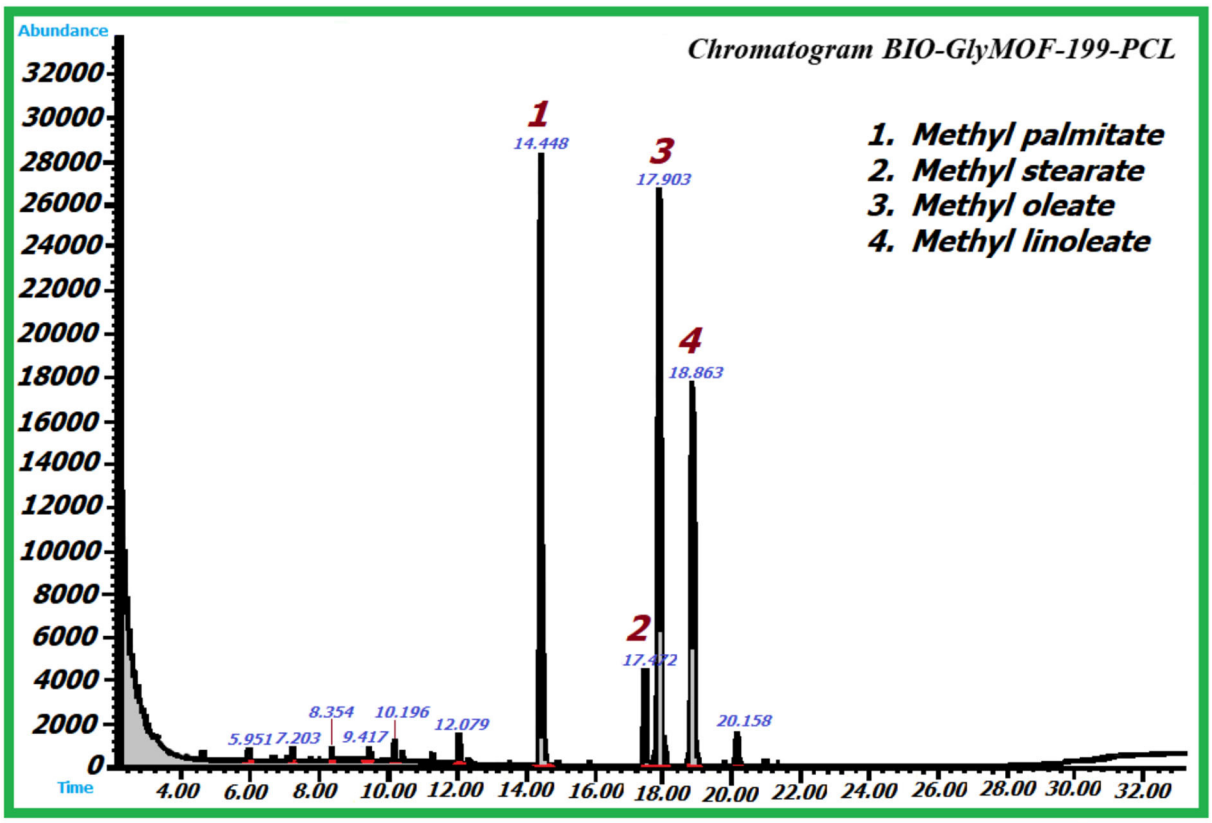

FIGURE 21
BIO-Gly@MOF-199-PCL biodiesel chromatogram synthesized by biocatalysis.

Nuclear magnetic resonance, starting materials, palm oil

Crude palm oil (OP), OP-BIOC commercial palm biodiesel, and biodiesels (BIO-MOF-199-PCL and BIO-Gly@MOF-199-PCL) synthesized by biocatalysis using MOF catalytic materials for this purpose MOF-199-PCL and Gly@MOF-199-PCL are analyzed using nuclear magnetic resonance (NMR). The ^{1}H NMR spectra for both OP palm oil and OP-BIOC commercial biodiesel are similar (Figures 22A,B), sharing signals at 5.3, 4.1, 2.1, 1.3, and 0.97 ppm; therefore, it can be inferred that the characteristics signals of the OP-BIOC are 3.6 and 2.4 ppm. These two signals present in OP-BIO indicate a compositional change, which is due to the fact that OP-BIOC is obtained industrially by complete transesterification of acylglycerides in oil methyl ester or FAME (palm Biodiesel). For these two types of biofuels, it follows that the proton signals between 4.0–4.4 and 5.1–5.4 ppm correspond to multiplets. It is noteworthy that signals between 7.1 and 7.2 ppm corresponding to singlet are only present in OP. These characteristic signals are the determinants to establish whether BIO-Gly@MOF-199-PCL corresponds to biodiesel-type components. The aforementioned signals are not observed in BIO-MOF-199-PCL, but in BIO-Gly@MOF-199-PCL (see Figures 23A,B). This may be due to the fact that BIO-Gly@MOF-199-PCL is made up of a mixture of FAMES and paraffin. It is also possible that the signals between 4.5 and 4.0 ppm indicate the structural incorporation of glycerin to the FAMEs and therefore glycerin is one more component of the biodiesel mixture due to a partial transesterification of palm oil (Calero et al., 2014; Ugur et al., 2014) by biocatalysts. This last conjecture is valid when attenuated signals are found around 2,800 and 3,500 cm^{-1} in the FTIR spectra of BIO-MOF-199-PCL and BIO-Gly@MOF-199-PCL.

In this scenario, it is concluded that biodiesel synthesized using MOF-199-PCL as a catalyst produces Ecodiesel, while biodiesel synthesized using Gly@MOF-199-PCL as a catalyst produces green diesel.

TABLE 10 Presence of free fatty acids in synthesized biodiesel.

Assigned compound	Biodiesel								Molecular formula
	OP-BIOC		CB-OP-BIO		BIO-MOF-199-PCL		BIO-Gly@MOF-199-PCL		
	Time	%Area	Time	%Area	Time	%Area	Time	%Area	
Tridecanoic acid	0	0	4.583	4.68	0	0	0	0	$C_{14}H_{26}O_4$
Meristic acid	0	0	5.931	4.18	0	0	0	0	$C_{14}H_{28}O_2$
Dotriacontanoic acid	0	0	6.660	2.87	0	0	0	0	$C_{32}H_{64}O_2$
Pentadecanoic acid	0	0	7.183	3.79	0	0	0	0	$C_{15}H_{30}O_2$
Palmitic acid	0	0	8.329	3.16	0	0	0	0	$C_{16}H_{32}O_2$
Heptadecanoic acid	0	0	9.392	5.28	0	0	0	0	$C_{17}H_{34}O_2$
Stearic acid	0	0	10.371	0.56	0	0	0	0	$C_{18}H_{36}O_2$

TABLE 11 Paraffins present in BIO-Gly@MOF-199-PCL.

Assigned compound	BIO-Gly@MOF-199-PCL		
	Biodiésel		
	Time	%Area	Molecular formula
Tetradecane	5.953	0.43	$C_{14}H_{30}$
Pentadecane	7.203	0.35	$C_{15}H_{32}$
Hexadecane	8.354	0.33	$C_{16}H_{34}$
Heptadecane	9.418	0.55	$C_{17}H_{36}$

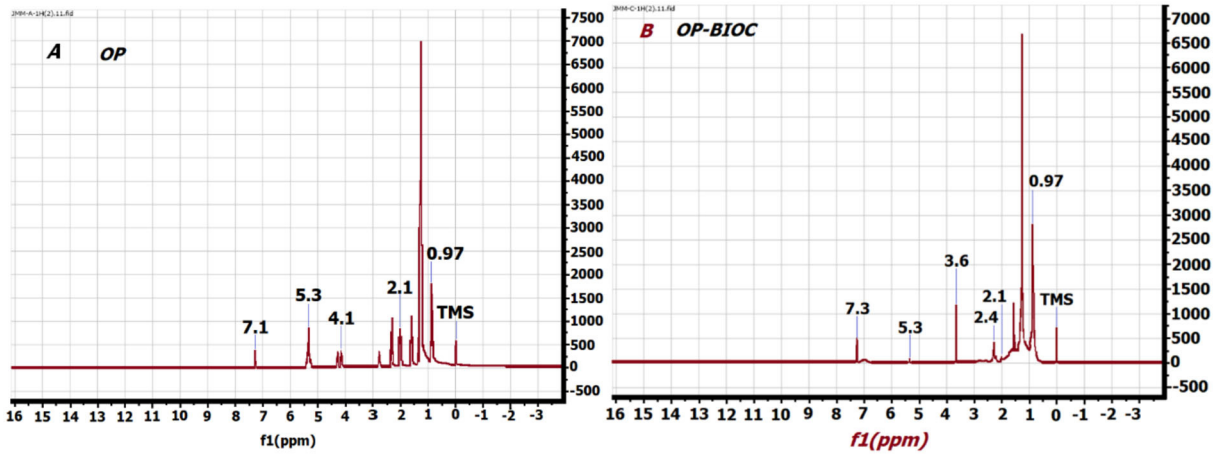

FIGURE 22
NMR spectrum: **(A)** OP, **(B)** OP-BIOC.

Conclusion

In this research, Ecodiesel formulation BIO-MOF-199-PCL and Green Diesel formulation BIO-Gly@MOF-199-PCL were synthesized, from the immobilization of *Pseudomonas cepacia* lipase on MOF-199 and Gly@MOF-199 from the thermal modification of MOF-199 impregnated with ethylene glycol, using African palm oil as raw material. The results showed that the MOF-199-PCL biocatalyst converts the acylglycerides present in palm oil into Ecodiesel, while the Gly@MOF-199-PCL biocatalyst converts the acylglycerides present in palm oil into green Diesel. The production of Ecodiesel is deducted by the

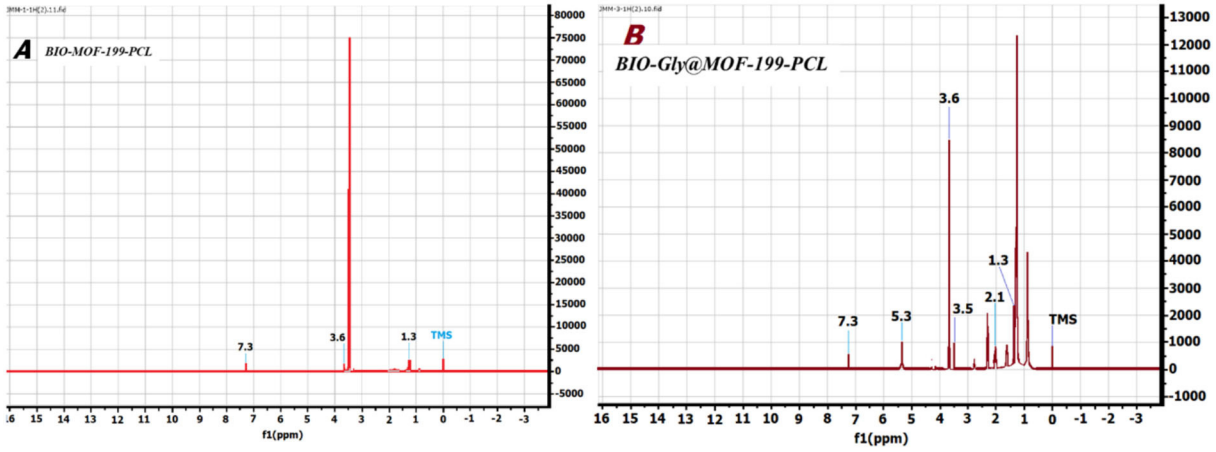

FIGURE 23
NMR spectrum: **(A)** BIO-MOF-199-PCL, **(B)** BIO-Gly@MOF-199-PCL.

presence of peaks at 921 and 2,800–3,500 cm^{-1} corresponding to a glycerol-like structure in the form of monoglycerides (López et al., 2022) in the FTIR, and the production of Ecodiesel and Green Diesel the presence of paraffins in the chromagram of BIO-Gly@MOF-199-PCL. The new biocatalysts MOF-199-PCL and Gly@MOF-199-PCL showed that they can carry out transesterification/yield reactions, a fact that is inferred by the formation of FAMEs and the absence of free fatty acids in the chromatograms of BIO biofuels. -MOF-199-PCL and BIO-Gly@MOF-199-PCL, but they are present in the biodiesel produced by basic catalysis CB-OP-BIO present, with the added value of not registering glycerin traits as evidenced in the synthesis of biodiesel by basic catalysis.

Limitations and recommendations

As a limitation of this research, it was found that it was necessary to perform a large number of experiments prior to finding the appropriate synthesis route to obtain the biocatalysts capable of conducting a reaction to synthesize quality biodiesel.

Therefore, one of the recommendations in this type of synthesis is to carry out a series of simulations prior to the synthesis. It is suggested, for example, to carry out a design of experiments to establish which variables influence the synthesis.

Data availability statement

The datasets presented in this article are not available. Requests for access to the datasets should be directed to jumoreno@uniandes.edu.co.

Author contributions

All authors listed have made a substantial, direct, and intellectual contribution to the work and approved it for publication.

Acknowledgments

The authors thank the Research and Postgraduate Committee-Faculty of Sciences of the Universidad de Los Andes, Colombia. Moreover, the authors appreciate the framework agreement between Universidad Nacional de Colombia and Universidad de los Andes (Bogotá, Colombia) under which this work was carried out. JM-P also thanks the Faculty of Sciences of the Universidad de Los Andes for an award, Number INV-2021-128-2257. Also, the authors extend their most sincere thanks to doctors: Laura Ibarra and Alexander Garay, members of the Gas Chromatography and NMR laboratory; Prof. Chiara Carazzone y Gerson López members of the laboratory of advanced techniques in natural products for allowing the use of the derivatization protocol described in Section Derivatization of palm oil for mass analysis, this derivatization route will soon be published in the multidisciplinary journal. JG expresses his gratitude to the Universidad de la Guajira, for its partial financial support to carry out this research.

Conflict of interest

The authors declare that the research was conducted in the absence of any commercial or financial relationships that could be construed as a potential conflict of interest.

Publisher's note

References

Al Obeidli, A., Salah, H. B., Al Murisi, M., and Sabouni, R. (2021). Recent advancements in MOFs synthesis and their green applications. *Int. J. Hydrogen Energy*. 47, 2561–2593. doi: 10.1016/j.ijhydene.2021.10.180

Angulo, B., Fraile, J. M., Gil, L., and Herrerías, C. I. (2020). Comparison of chemical and enzymatic methods for the transesterification of fatty ethyl esters of residual fish oil with different alcohols. *ACS Omega* 5, 1479–1487. doi: 10.1021/acsomega.9b03147

Calero, J., Luna, D., Luna, C., Bautista, F. M., Romero, A. A., Posadillo, A., et al. (2020). Optimization by response surface methodology of the reaction conditions in 1, 3-selective transesterification of sunflower oil, by using CaO as heterogeneous catalyst. *Mol. Catal.* 484, 110804. doi: 10.1016/j.mcat.2020.110804

Calero, J., Luna, D., Sancho, E. D., Luna, C., Bautista, F. M., Romero, A. A., et al. (2014). Development of a new biodiesel that integrates glycerol, by using CaO as heterogeneous catalyst, in the partial methanolysis of sunflower oil. *Fuel* 122, 94–102. doi: 10.1016/j.fuel.2014.01.033

Chang, M. Y., Chan, E. S., and Song, C. P. (2021). Biodiesel production catalyzed by low-cost liquid enzyme Eversa® Transform 2.0: effect of free fatty acid content on lipase methanol tolerance and kinetic model. *Fuel* 283, 119266. doi: 10.1016/j.fuel.2020.119266

Chaudhari, V. D., Jagdale, V. S., Chorey, D., and Deshmukh, D. (2021). Combustion and spray breakdown characteristics of biodiesel for cold start applications. *Clean. Eng. Technol.* 5, 100285. doi: 10.1016/j.clet.2021.100285

Chen, M., Chen, J., Liu, Y., Liu, J., Li, L., Yang, B., et al. (2019). Enhanced adsorption of thiophene with the GO modified bimetallic organic framework Ni-MOF-199. *Colloids Surf. A Physicochem. Eng. Aspects* 578, 123553. doi: 10.1016/j.colsurfa.2019.06.019

Deshmukh, M. A., Celiesiute, R., Ramanaviciene, A., Shirsat, M. D., and Ramanavicius, A. (2018). EDTA_PANI/SWCNTs nanocomposite modified electrode for electrochemical determination of copper (II), lead (II) and mercury (II) ions. *Electrochim. Acta* 259, 930–938. doi: 10.1016/j.electacta.2017.10.131

Díaz-Duran, A.K., and Roncaroli, F. (2021). The influence of particle size and shape in cobalt 2-methylimidazolate polymers on cata-lytic properties. *Eur. J. Inorg. Chem.* 28, 2830–2839. doi: 10.1002/ejic.202100255

Dong, X., Su, Y., Lu, T., Zhang, L., Wu, L., and Lv, Y. (2018). MOF-derived dodecahedra porous Co_3O_4: an efficient cataluminescence detection material for H2S. *Sensors Actuat. B: Chem.* 258, 349–357. doi: 10.1016/j.snb.2017.11.090

Dong, Z., Mi, Z., Shi, W., Jiang, H., Zheng, Y., and Yang, K. (2017). High pressure effects on Cu-BTC hydrate investigated by vibrational spectroscopy and synchrotron X-ray diffraction. *RSC Adv.* 7, 55504–55512. doi: 10.1039/C7RA11843K

Fuller, M. P., and Griffiths, P. R. (1978). Diffuse reflectance measurements by infrared Fourier transform spectrometry. *Anal. Chem.* 50, 1906–1910. doi: 10.1021/ac50035a045

Guerrini, L. (2009). Functionalization of metal nanoparticles for the detection of persistent organic pollutants by surface-enhanced Raman spectroscopy. *Anal. Chim. Acta* 624, 286–293 doi: 10.1021/ac801709e

Heiden, R. W., Schober, S., and Mittelbach, M. (2021). Solubility limitations of residual steryl glucosides, saturated monoglycerides and glycerol in commercial biodiesel fuels as determinants of filter blockages. *J. Am. Oil Chem. Soc.* 98, 1143–1165. doi: 10.1002/aocs.12547

Jaecker-Voirol, A., Durand, I., Hillion, G., Delfort, B., and Montagne, X. (2008). Glycerin for new biodiesel formulation. *Oil Gas Sci. Technol.* 63, 395–404. doi: 10.2516/ogst:2008033

Kovacic, F., Babic, N., Krauss, U., and Jaeger, K. (2019). Classification of lipolytic enzymes of bacteria. *Aerob. Util. Hydrocarbons Oils Lipids* 24, 255–289. doi: 10.1007/978-3-319-50418-6_39

Krishnasamy, A., and Bukkarapu, K. R. (2021). A comprehensive review of biodiesel property prediction models for combustion model studies. *Fuel* 302, 121085. doi: 10.1016/j.fuel.2021.121085

Kumar, A., Gudiukaite, R., Gricajeva, A., Sadauskas, M., Malunavicius, V., Kamyab, H., et al. (2020). Microbial lipolytic enzymes: promising energy efficient biocatalysts in bioremediation. *Energy*. 192, 116674. doi: 10.1016/j.energy.2019.116674

Lemke, K., Lemke, M., and Theil, F. (1997). A three-dimensional predictive active site model for lipase from *Pseudomonas cepacia*. *J. Org. Chem.* 62, 6268–6273. doi: 10.1021/jo970838d

Li, L., Liu, X. L., Geng, H. Y., Hu, B., Song, G. W., and Xu, Z. S. (2013). A MOF/graphite oxide hybrid (MOF: HKUST-1) material for the adsorption of methylene blue from aqueous solution. *J. Mater. Chem. A* 1, 10292–10299. doi: 10.1039/C3TA11478C

López, J. M., Flores, F. P., Rosales, E. C., Muñoz, E. O., Hernández-Anzaldo, S., Lima, H. V., et al. (2022). Theoretical and experimental study of the liquid-liquid balance to refine crude glycerol obtained as a by-product in the production of biodiesel. *Adv. Chem. Eng. J.* 10, 100257. doi: 10.1016/j.ceja.2022.100257

Milano, J., Shamsuddin, A. H., Silitonga, A. S., Sebayang, A. H., Siregar, M. A., Masjuki, H. H., et al. (2022). Tribological study on the biodiesel produced from waste cooking oil, waste cooking oil blend with *Calophyllum inophyllum* and its diesel blends on lubricant oil. *Energy Rep.* 8, 1578–1590. doi: 10.1016/j.egyr.2021.12.059

Monteiro, R. R., Virgen-Ortiz, J. J., Berenguer-Murcia, A., da Rocha, T. N., dos Santos, J. C., Alcantara, A. R., et al. (2021). Biotechnological relevance of the lipase A from *Candida antárctica*. *Catalysis Today* 362, 141–154. doi: 10.1016/j.cattod.2020.03.026

Shomal, R., Du, W., and Al Zuhair, S. (2022). Immobilization of lipase on metal-organic frameworks for biodiesel production. *J. Environ. Chem. Eng.* 2022:107265. doi: 10.1016/j.jece.2022.107265

Shomal, R., Ogubadejo, B., Shittu, T., Mahmoud, E., Du, W., and Al-Zuhair, S. (2021). Advances in enzyme and ionic liquid immobilization for enhanced in MOFs for biodiesel production. *Molecules* 26, 3512. doi: 10.3390/molecules26123512

Tranchemontagne, D. J., Hunt, J. R., and Yaghi, O. M. (2008). Room temperature synthesis of metal-organic frameworks: MOF-5, MOF-74, MOF-177, MOF-199, and IRMOF-0. *Tetrahedron* 64, 8553–8557. doi: 10.1016/j.tet.2008.06.036

Ugur, A., Sarac, N., Boran, R., Ayaz, B., Ceylan, O., and Okmen, G. (2014). New lipase for biodiesel production: partial purification and characterization of LipSB 25-4. *Int. Scholarly Res. Not.* 2014:289749. doi: 10.1155/2014/289749

Wang, H., Li, T., Li, J., Tong, W., and Gao, C. (2019). One-pot synthesis of poly (ethylene glycol) modified zeolitic imidazolate frame-work-8 nanoparticles: Size control, surface modification and drug encapsulation. *Colloids Surf. A Physicochem. Eng. Aspects* 568, 224–230. doi: 10.1016/j.colsurfa.2019.02.025

Woolley, E. M., Tomkins, J., and Hepler, L. G. (1972). Ionization constants for very weak organic acids in aqueous solution and apparent ionization constants for water in aqueous organic mixtures. *J. Solution Chem.* 1, 341–351. doi: 10.1007/BF00715992

Zhao, S., Zhang, Y., Wu, Y., Zhang, L., Hu, H., and Jin, L. (2022). ZIF-derived hierarchical pore carbons as high-performance catalyst for methane decomposition. *J. Energy Inst.* 100, 197–205. doi: 10.1016/j.joei.2021.11.015

Zhen, X., Wang, Y., and Liu, D. (2020). Biobutanol as a new generation of clean alternative fuel for SI (spark ignition) and CI (compression ignition) engines. *Renew. Energy* 147, 2494–2521. doi: 10.1016/j.renene.2019.10.119